THE IMPACT OF HYPOPHOSPHATEMIA ON CHONDROCYTE FATE

A Thesis

by

VIJAYA KONDRU

Submitted to the Office of Graduate and Professional Studies of

Texas A&M University

in partial fulfillment of the requirements for the degree of

MASTER OF SCIENCE

Chair of Committee,	Jerry Feng
Committee Members,	Lynne Opperman
	Yan Jing
Head of Department,	Larry Bellinger

August 2017

Major Subject: Oral Biology

ABSTRACT

Dentin Matrix Protein 1(DMP1) is a non-collagenous phosphoprotein, belonging to the Small Integrin **s**mall integrin-binding l**i**gand, N-linked glycoprotein (SIBLING) family, the deficiency or mutation of which results in Autosomal Recessive Hypophosphatemic Rickets, as evidenced by the accumulation of hypertrophic chondrocytes, resulting in immature or "premature" bone formation and mineralization.

We employed cell lineage tracing (AggcretoDMP1$^{-/-}$) together with other techniques to analyze the skeletal phenotype in DMP1 null mice at P10; these mice had shortened long bones and decreased circulatory levels of phosphate. While exogenous phosphate administration, in vitro, appeared to rescue the phenotype, we observed increased expressions of collagen 1 and osteopontin, together with high alkaline phosphatase activity (ALP) in the bone matrix, suggesting that these "accumulated" cells are actively differentiating into bone cells and secreting bone matrix; moreover, these bone cells were immature, and actively dividing, as indicated by decreased sclerostin (SOST) expression and increased Ki67 levels, respectively. However, while there was no apparent change in collagen 2 (Col2) and collagen 10 (Col10) expression, and Endomucin activity, Osterix and Runx2 levels were higher in the DMP1 control than in the KO.

In conclusion, there is increased chondrogenesis in a "hypophosphate" environment in DMP1 null mice; here, hypertrophic chondrocytes "persist" and differentiate rapidly into

immature bone cells (they do not apoptose as previously believed). While exogenous phosphate positively influenced the secondary ossification center in long bones, further studies at different time points are necessary to demonstrate such an effect. Moreover, to demonstrate the influence of phosphate rich diet on phenotype, cell lineage tracing studies are warranted to study the cell transformation from chondrocytes to bone cells.

DEDICATION

I want to dedicate my thesis to my husband Sekhar Molli, my parents Narasimha Murthy Kondru & Satyavathi Kondru, my in-laws Ramana Murthy Molli & Vijaya Ratna Kumari Molli, and brother, Praveen Kondru for their support and encouragement in all my endeavors. I want to thank all my colleagues and friends for being there for me.

ACKNOWLEDGEMENTS

I want to thank my committee chair, Dr. Jerry Feng, and committee members, Dr. Lynne Opperman and Dr. Yan Jing, for their guidance and encouragement towards my thesis. I also want to thank Dr. Kathy Svoboda, who guided me throughout my master's.

I want to thank all my colleagues, Ke Wang, Jun Wang, Chaoyuan Li, Ying Liu, Tian Meng, Liang and Jingya Wang, who have helped me and made a comfortable environment while working. I am also grateful to my friends, Neelam Ahuja, Mahesh Rao, Rajay Kamath and Priyam Jani, who stood by me always. Lastly, I want to thank all the biomedical sciences faculty and staff at Texas A & M University College of Dentistry.

CONTRIBUTORS AND FUNDING SOURCES

Contributors

This work was supervised by my thesis committee consisting of Dr. Jerry Feng and Dr. Lynne A. Opperman from the Department of Biomedical Sciences at Texas A&M University College of Dentistry, and Dr. Yan Jing from the Department of Orthodontics, at Texas A&M University College of Dentistry.

All work for the thesis was completed independently by the student under the advisement of Dr. Jerry Feng from the Department of Biomedical Sciences at Texas A&M University College of Dentistry.

Funding Sources

This work was made possible in part by:

1.NIH Grant Number RO1 DE025659

2.The Office of Associate Dean for Research and Graduate studies

3.The Department of Biomedical Sciences at Texas A&M University College of Dentistry.

Its contents are solely the responsibility of the authors and do not necessarily represent the official views of the NIH.

NOMENCLATURE

DMP1	Dentin Matrix Protein 1
FGF23	Fibroblast Growth Factor
PHEX	Phosphate-regulating gene with Homologies to Endopeptidases on the X chromosome
IHH	Indian Hedge Hog
PTHRP	Parathyroid hormone related peptide
PPR Signaling	Parathyroid hormone and Parathyroid hormone related peptide signaling
ARHR	Autosomal Recessive Hypophosphatemic Rickets
Cbfa1	core-binding factor subunit alpha-1
Runx2	Runt-related transcription factor 2
Dmp1- (KO)	Dentin Matrix Protein Gene Knock out
Aggcreto	Aggrecan-Cre ^{ERT2} and Rosa26 ^{tdTomato}
EDTA	Ethylene Diamine Tetra-acetic Acid
TRAP	Tartrate-resistant acid phosphatase
ALP	Alkaline Phosphatase
COL1	Collagen 1
COL2	Collagen 2
COL10	Collagen 10
OPN	Osteopontin

OSX	Osterix
EDU	5-Ethynyl-2´-deoxyuridine
DAPI	4',6-diamidino-2-phenylindole
IHC	Immuno Histo-Chemistry
IF	Immunofluorescence
X–ray	X-radiation
NaoH	Sodium hydroxide
NIH	National Institute of Health
OCT	Optimal cutting temperature compound
PBS	Phosphate-buffered saline
SEM	Scanning electron microscopy
SIBLINGs	Small Integrin-Binding Ligand N-liked glycoproteins
TGF-β1	Transforming growth factor beta-1
Pi	Inorganic Phosphate
IACUC	Institution of Animal Care and Use Committee
PFA	Paraformaldehyde
PBST	Phosphate Buffered Saline with Tween 20
ALP	Alkaline Phosphatase
BV/TV	Bone Volume / Total Volume
mM	Milli Molar
βGP	Beta Glycero Phosphate

TABLE OF CONTENTS

Page

LIST OF FIGURES

Page

CHAPTER I

INTRODUCTION AND LITERATURE REVIEW

Human bones, for the most part, form by endochondral ossification wherein cartilage is replaced by bone, a complex process involving a definite sequence of differentiation of chondrocytes in the growth plate of long bones. To further elaborate, resting chondrocytes in the germinal zone of the growth plate begin to proliferate, then transform into prehypertrophic, and then hypertrophic chondrocytes, followed by calcified cartilage formation and its invasion by bone marrow. The cartilage is then resorbed and eventually replaced by subchondral bone (A, 1991; Kronenberg, 2003). These steps are regulated by many transcription factors and signaling pathways, under the influence of growth factors, hormones, and their specific receptors (Goldring, Tsuchimochi, & Ijiri, 2006)

Although the current dogma that hypertrophic chondrocytes undergo apoptosis is still widely held (de Crombrugghe, Lefebvre, & Nakashima, 2001), recent evidence suggests that these chondrocytes directly transform into bone cells, rather than undergoing apoptosis, during endochondral ossification (Jing et al., 2015). However, this emerging concept warrants further elucidation on the genetic and molecular underpinnings that ultimately influence such fate.

The regulation of chondrogenesis is complex and involves several molecular factors such as transcription factors, signaling molecules and epigenetic factors.

Indian hedgehog (Ihh) is one of several factors that regulates chondrogenesis. Expressed by prehypertrophic chondrocytes, it accelerates chondrocytic differentiation, an effect that is counter-balanced by FGF23. Parathyroid hormone-related peptide (PTHRP), another potent factor, maintains chondrocyte proliferation rate (J. Guo, Chung, Kondo, Bringhurst, & Kronenberg, 2002; Kobayashi et al., 2002) by acting through the PTHRP receptor (Chung, Lanske, Lee, Li, & Kronenberg, 1998; Karaplis et al., 1994; Lanske et al., 1996) via the secondary messenger cAMP pathway. The latter in turn modulates gene expression by PKA-dependent phosphorylation of the CREB gene at Ser 133(Gonzalez & Montminy, 1989)which ultimately affects Ptch expression in proliferating chondrocytes, unlike Ihh. Deletion of the CREB gene results in death of the neonate owing to defects in lung maturation(Rudolph et al., 1998). Activity of PTH/PTHrP (PPR) signaling is also dependent on Ihh in blocking premature hypertrophic differentiation of columnar chondrocytes (Figure 1,2) (Chung, Schipani, McMahon, & Kronenberg, 2001; Lanske et al., 1996; Vortkamp et al., 1996). In addition, Ihh helps in stimulating the differentiation of periarticular (resting) chondrocytes into proliferating chondrocytes, a process independent of PTHRP (Karp et al., 2000).

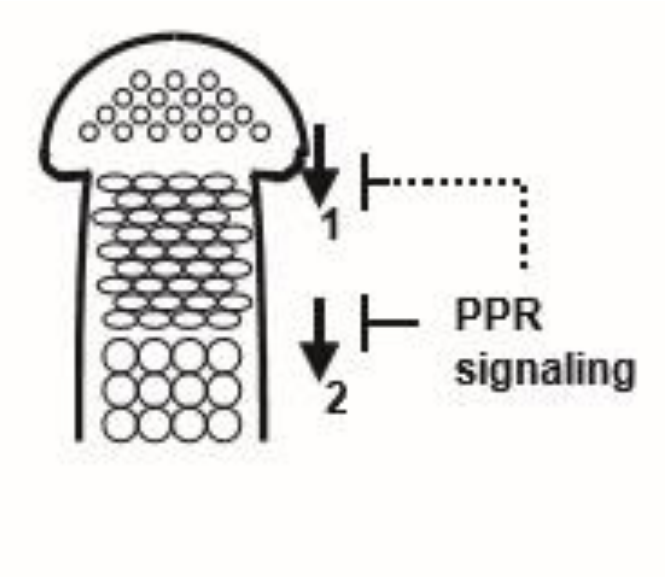

Figure 1: PPR signaling: PPR signaling controls negatively the differentiation of periarticular chondrocytes to columnar chondrocytes (arrow 1) and it also blocks the terminal differentiation of columnar chondrocytes (arrow 2). Reprinted with permission from Kobayashi et al…2002

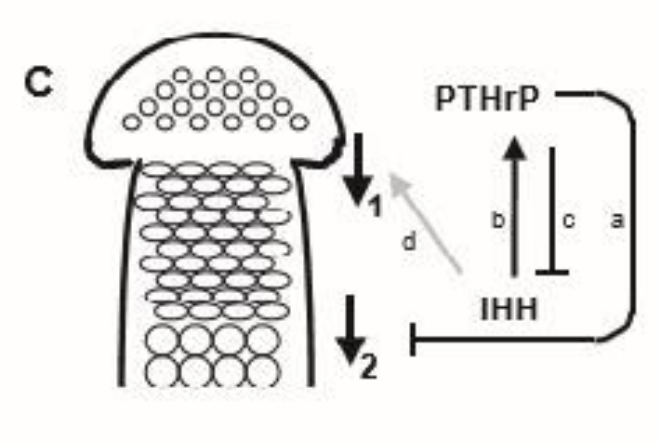

Figure 2: PTHrP -IHH feedback loop: a**.** Premature hypertrophic chondrocyte differentiation is directly blocked by PTHrP signaling. b**.** PTHrP is positively regulated by IHH in the periarticular region. c. PTHrP positively influences the columnar formation of chondrocytes between periarticular region and the IHH domain'**s.** d. Ihh action stimulates early chondrocyte proliferation and differentiation, thereby increasing their numbers. Reprinted with permission from Kobayashi et al…2002

Of significance are BMPs, members of the TGFβ superfamily that play a major role in chondrocyte proliferation and differentiation (Massague, 2012; Massague & Wotton, 2000). BMP'S are essential for early limb development, in addition to being found in the perichondrium (BMP – 2,3,4,5,7), and proliferative (BMP – 7) and hypertrophic chondrocytes (BMP – 2,6)(Kugimiya et al., 2005; Shen et al., 2015). Functionally, BMPs induce the phosphorylation of Smads after they bind to their serine–threonine kinase activity cell-surface receptors. Following nuclear translocation, smads bind to their target genes(Li et al., 2003). There are mainly two types of BMP receptors - BmpR-IA and BmpR-IB. While BmpR-IB activity is necessary in the initial stages of chondrogenesis and in regulating apoptosis(Graham, Francis-West, Brickell, & Lumsden, 1994; Zou & Niswander, 1996), BmpR-IA is required in the later stages of chondrogenesis

(prehypertrophic chondrocytes) and its signaling through the perichondrium(Kingsley, 1994) regulates Ihh–PTHRP signaling axis.

Further, Wnt/β-catenin signaling is required for normal cartilage and bone formation(Day, Guo, Garrett-Beal, & Yang, 2005). Intercellular cell signaling between or within condensed mesenchymal cells (from which osteoblasts and chondrocytes develop) play an important role in cell differentiation and Wnt expression in different stages of endochondral ossification suggests its role in cellular differentiation(X. Guo et al., 2004; Kato et al., 2002; Parr, Shea, Vassileva, & McMahon, 1993). Wnt signaling results in elevated cytoplasmic β–catenin and its subsequent translocation to the nucleus to begin transcription of TCF/LEF transcription factor family members (Logan & Nusse, 2004) to cause osteoblast differentiation, and inhibiting the activity of β–catenin causes commitment of cells to a chondroblastic lineage (Figure 3).

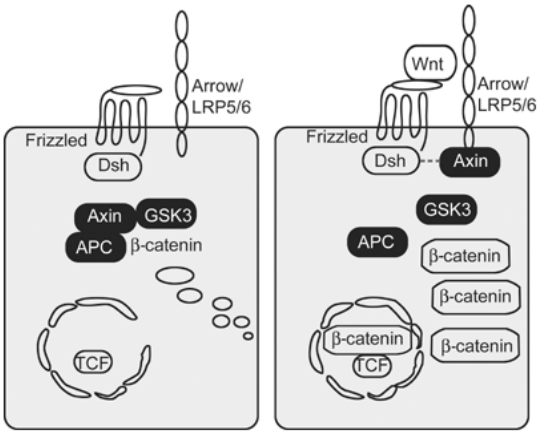

Figure 3: Wnt Signaling: Left panel shows degradation of βcatenin through interaction of Axin, GSK3, APC without Wnt signaling. Right panel shows binding of Wnt to cell surface Frizzled receptor complex which transduce a signal to Axin, GSK3, APC and to Dishevelled (Dsh). The result is that βcatenin degradation is inhibited and it accumulates in cytoplasm and nucleus. Then it interacts with TCF and causes / controls transcription. Reprinted with permission from Roel Nusse et al…2005.

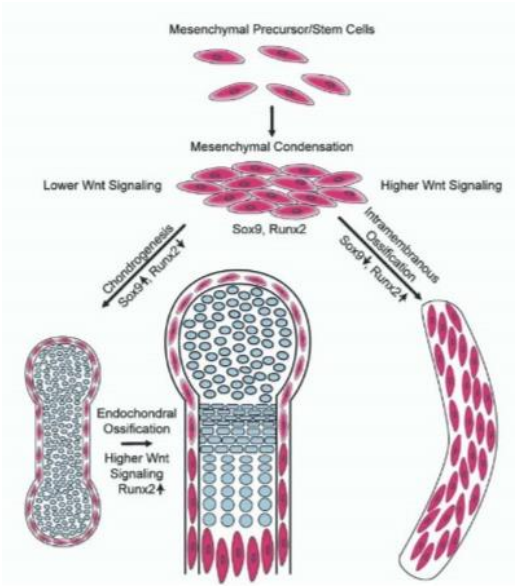

Figure 4: Wnt Signaling and cell differentiation: Mesenchymal precursor stem cells and condensations which has ability to differentiate in to cartilage and bone are labelled pink, the chondrocytes blue. In the precursor cells determined to form bone (intramembranous ossification) there is higher Wnt signaling, Runx2 expression is upregulated and Sox 9 is downregulated. In the precursor cells determined to form cartilage template first, followed by bone (endochondral ossification), there is lower Wnt signaling, Sox 9 upregulation and Runx2 downregulation. Later Wnt signaling is upregulated, Runx2 is upregulated from perichondrium, thereby contributing to bone formation. Reprinted with permission from Day et al.....2005

Transcription factors such as cbfa1/ Runx2, which belongs to runt (Ducy, Zhang, Geoffroy, Ridall, & Karsenty, 1997) family, is known to stimulate osteoblast differentiation,(Komori et al., 1997) . Recent studies show that cbfa1 also stimulates hypertrophic chondrocyte maturation, and contributes to chondrocyte differentiation, as cbfa1 homozygous mutations were shown to develop phenotypes completely devoid of bone, while heterozygous mutations have been shown to develop cleidocranial dysplasia (Mundlos, Huang, Selby, & Olsen, 1996). In addition, they developed cartilage anomalies

causing chondrodysplasias in mice. (Ducy et al., 1997; Enomoto-Iwamoto, Enomoto, Komori, & Iwamoto, 2001; Leboy et al., 2001; Otto et al., 1997). Cbfa1 is a positive regulator of chondrogenesis and is known to exert its effect through 3 different mechanisms: first, by direct expression in prehypertrophic and hypertrophic chondrocytes; second, through indirect signaling by perichondral cells; third, through a combination of the above i.e. mechanisms 1 and 2(Kim, Otto, Zabel, & Mundlos, 1999).

Sox-9, another important transcription factor expressed in proliferative and pre-hypertrophic chondrocytes, determines cell fate during early chondrogenesis. Sox-5 & Sox-6 are also co expressed with Sox 9 in chondroprogenitor cells(Lefebvre, Huang, Harley, Goodfellow, & de Crombrugghe, 1997). Inactivation of Sox-9 before mesenchymal condensation disturbs not only the cartilage formation but also endochondral ossification(Akiyama, Chaboissier, Martin, Schedl, & de Crombrugghe, 2002; Bi, Deng, Zhang, Behringer, & de Crombrugghe, 1999) by disrupting Runx2 transcript which is necessary for osteoblast differentiation. It acts by binding to specific sequences in the collagen 2 α 1 and collagen 2 α XI gene and can enhance the activity in non chondrocytic areas too.

Apart from transcription factors, gene transcription also depends on histone modifications in cartilage development (Kubicek & Jenuwein, 2004; Martin & Zhang, 2005; Strahl & Allis, 2000). Tri-methylation of lysine 27 on histone H3 (H3K27me3) signifies the transcriptional regression and is established by enhancer of zeste homolog 2 (EZH2), a

core subunit of the polycomb repressive complex 2 (PRC2) (Czermin et al., 2002; Muller et al., 2002). Previous studies have identified Jumonji domain-containing proteins UTX (KDM6A) and JMJD3 (KDM6B) as H3K27me3-specific demethylases, implying that polycomb mediated gene silencing can be regulated and is reversible (Agger et al., 2007; De Santa et al., 2007; Hong et al., 2007). Histone deacetylase HDAC4 and H3K9 methyltransferase ESET inhibit chondrocyte hypertrophy in vivo but their role in cellular proliferation is not known(Vega et al., 2004; D. Yang, Okamura, Nakashima, & Haneji, 2013). Genetic and biochemical studies show that JMJD3 promotes both proliferation and hypertrophy by interacting with Runx2 as JMJD3 cannot bind to DNA by itself; so Runx2 helps in recruiting JMJD3 to the specific site (Figure 5). JMJD3 interacts with N – terminus of Runx2 to enhance its action, thereby helping in chondrocyte differentiation. Hence, JMJD3 acts as an important epigenetic factor in cartilage development(F. Zhang et al., 2015).

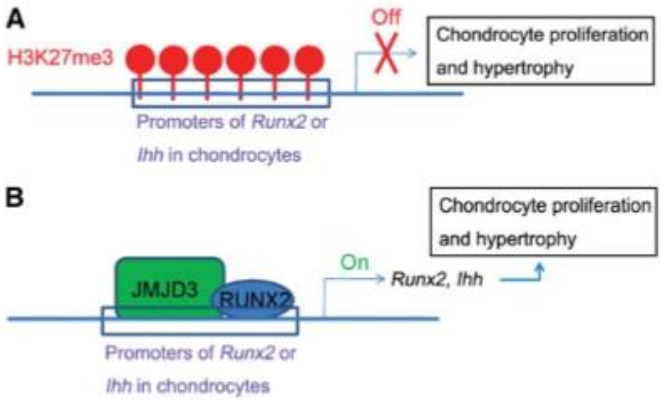

Figure 5: JMJD3 and Endochondral bone formation: a.H3K27me3 modification enables the repression of transcription of target gene Runx2 and Ihh in chondrocytes.b. JMJD3 counteracts the H3K27me3 modification and facilitates the transcription of Runx2 in chondrocytes. Reprinted with permission from Zhang F et al……2015

Gsα, a heterotrimeric stimulatory protein which binds to adenyl cyclase to form Cyclic AMP, is encoded by the GNAS gene in mice and its mutation in humans results in Albright Hereditary Osteodystrophy (Bastepe et al., 2004; Mantovani, Spada, & Elli, 2016; Turan & Bastepe, 2015) This protein is thought to be a negative regulator of chondrogenesis as mutations in this gene causes severe epiphyseal defects and growth plate retardation. It is thought to exert its action by acting on the PTHRP-PTH receptor in growth plates(Sakamoto, Chen, Kobayashi, Kronenberg, & Weinstein, 2005).

Matrilins (MATN1, MATN2, MATN3, MATN4) (Klatt et al., 2000) belongs to a family of four non-collagenous proteins that share similar structural motifs (Deak, Wagener, Kiss, & Paulsson, 1999; Klatt et al., 2000). While MATN1 and MATN3 are specific to

cartilage(Wagener, Kobbe, & Paulsson, 1997), MATN2 and MATN4 have a wider distribution. MATN3 has the simplest structure among other matrilin members. It contains a single vonWillebrand factorA (vWFA) domain, a C-terminal coiled-coil domain, and four epidermal growth factor (EGF)-like domains which mediates oligomerization(Wagener et al., 1997) (Figure 6). It is thought to play a structural role by binding to cartilaginous ECM proteins Col II and Col IX(Fresquet et al., 2007). It also regulates chondrogenesis via an interleukin receptor antagonist-dependent mechanism(Jayasuriya, Goldring, Terek, & Chen, 2012; Pei, Luo, & Chen, 2008). MATN3 inhibits premature hypertrophy by binding to the BMP2 receptor and decreasing SMAD 1 activity (Figure 7).

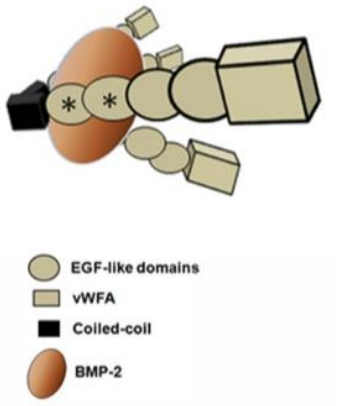

Figure 6: MATN3 and BMP-2 interaction: Diagram represents that the coiled coil domain and 2 EGF like domains of MATN3 are necessary for BMP-2 signal inhibition. Reprinted with permission from Xu Yang et al….2014

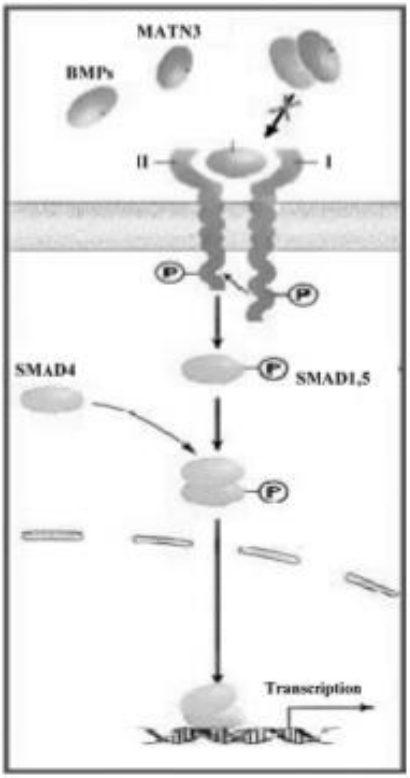

Figure 7: MATN3 chondrocyte hypertrophy regulation through BMP-2 signaling: MATN3 binds to BMP-2 via the EGF domains in the coiled-coil domain. This binding inhibits the activation of Smad 1, its translocation in to the nucleus and thereby binding with Col10 gene with Runx2 transcriptional activity, finally inhibiting chondrocyte hypertrophy. Reprinted with permission from Xu Yang et al….2014

The role of phosphates in mineralization of cartilage is well-known. Optimal phosphate concentration is necessary to maintain sufficient circulatory levels and in the initial formation of hydroxyapatite crystals. Classically, whereas phosphate homeostasis is controlled by parathyroid hormone and vitamin D by regulating its intestinal absorption and its reabsorption in the kidneys(Schiavi & Kumar, 2004; Tenenhouse, 1997). FGF23 is a phosphaturic hormone, which is mainly produced by osteocytes in bone. FGF23 is

present in many tissues like liver, thymus, parathyroid, bone, heart(Shimada et al., 2001; Yamashita, Yoshioka, & Itoh, 2000),(Saito et al., 2003) thereby contributing to phosphate balance in the body. Thus, taken together, these implicate bone as an 'endocrine organ' that functions via a complex bone-kidney axis.

DMP1 is a non-collagenous phosphoprotein of the SIBLING family(Fisher LW, 2003), a deficiency or mutation of which leads to cartilage defects in mice and Autosomal Recessive Hypophosphatemic Rickets (ARHR) in humans (Ye et al., 2005), the latter being associated with increased levels of FGF23, thereby resulting in renal phosphate wasting (Feng et al., 2006)**.** Mutations in (PHEX) phosphate regulating gene with homologies to endopeptidases on the X chromosome) have also been associated with X-linked hypophosphatemia (Makras, Hamdy, Kant, & Papapoulos, 2008; Sabbagh, Carpenter, & Demay, 2005; Yuan et al., 2008)**.** Both these conditions occur through a common pathway of decreased phosphate levels in blood secondary to increased FGF23 levels. Further, FGF23 mutations are known to cause Autosomal Dominant Hypophosphatemic Rickets (Liu et al., 2008) by decreasing the proliferating chondrocytes and increasing the differentiation to hypertrophic chondrocytes, thereby causing achondroplasia(Colvin, Bohne, Harding, McEwen, & Ornitz, 1996; Deng, Wynshaw-Boris, Zhou, Kuo, & Leder, 1996). Regardless, all the three mutations lead to defects in cartilage and bone formation and exhibit low phosphate levels in circulation and show expanded growth plate, decreased apoptosis of the hypertrophic chondrocyte zone(Sabbagh et al., 2005). Previous studies conducted in rachitic rats showed that

phosphate is preferentially sequestrated relative to calcium in the hypertrophic zone(Howell, Pita, Marquez, & Madruga, 1968) and the size of inorganic phosphate crystals determines the degree of conversion of demineralized to mineralized cartilage(Bingham & Raisz, 1974; Kakuta, Golub, & Shapiro, 1985). Studies done in calcium sensing receptor knock out mice, that exhibited hyperparathyroidism due to impaired calcium sensing, showed hypophosphatemia and rachitic changes despite hypercalcemia(Tu et al., 2003). All the above studies clearly indicate a correlation between low phosphate levels and rachitic changes in mice.

Stanniocalcin, a glycoprotein initially identified in fish (Wagner, Hampong, Park, & Copp, 1986), regulates calcium metabolism (Wagner, Milliken, Friesen, & Copp, 1991) by preventing hypercalcemia and causing phosphate reabsorption through kidneys (Lu, Wagner, & Renfro, 1994). Following its identification in mice and humans(Chang et al., 1995; Olsen et al., 1996) this protein was shown to have a more profound effect on phosphate (Madsen et al., 1998; Wagner et al., 1997) than calcium metabolism via sodium-dependent phosphate transporter activity. It is distributed throughout the body in the lungs, heart, bone, kidney, thyroid, and intestine) (De Niu et al., 2000; Wagner, Guiraudon, Milliken, & Copp, 1995; Worthington et al., 1999). Previous phosphate studies indicate that high intracellular phosphate levels induce chondrocyte apoptosis(Magne et al., 2003; Mansfield, Rajpurohit, & Shapiro, 1999; Mansfield, Teixeira, Adams, & Shapiro, 2001; Rajpurohit, Mansfield, Ohyama, Ewert, & Shapiro, 1999) by activating caspase 9 (Sabbagh et al., 2005) and disrupting the mitochondrial cell

membrane. Increased phosphate levels also inhibit cbfa1, thereby inhibiting chondrogenesis (Enomoto et al., 2000; Fujita et al., 2001; Hoshi, Komori, & Ozawa, 1999). Stanniocalcin also inhibits FGF23, causing increased phosphate uptake by chondrocytes via Na–II pi transporter activity, thereby inhibiting chondrogenesis at the growth plate.

Previous invitro studies confirmed that 7Mm phosphate concentrate in cultures is sufficient to induce caspase 9 mitochondrial apoptosis of hypertrophic chondrocytes(Mansfield et al., 1999) and it is differentiation dependent as the same concentration did not induce apoptosis in chondrocytes where the terminal differentiation did not take place(Sabbagh et al., 2005). This inhibition was due to lack of vascular invasion suggesting that phosphate is necessary in every step of endochondral ossification (Zalutskaya, Cox, & Demay, 2009).

CHAPTER II

MAJOR HYPOTHESIS

The human appendicular skeleton forms by endochondral ossification wherein cartilage is replaced by bone, a complex process involving a definite sequence of differentiation of chondrocytes in the growth plate of long bones. To further elaborate, resting chondrocytes in the germinal zone of the growth plate begin to proliferate, then transform into prehypertrophic, and then hypertrophic chondrocytes, followed by calcified cartilage formation and its subsequent invasion by bone marrow. The cartilage is then resorbed and eventually replaced by subchondral bone (A, 1991; Kronenberg, 2003). These steps are regulated by many transcription factors and signaling pathways, under the control of growth factors and hormones, and their specific receptors (Goldring et al., 2006). While the current dogma maintains that hypertrophic chondrocytes undergo apoptosis (de Crombrugghe et al., 2001), recent evidence suggests that these chondrocytes directly transform into bone cells, rather than undergoing apoptosis during endochondral ossification (Jing et al., 2015). However, further elucidation on the genetic and molecular underpinnings that ultimately influence such fate, in endochondral ossification, is warranted.

2.1 Molecular Biology of Chondrocytes

The regulation of chondrogenesis is complex and involves several molecular factors such as transcription factors, signaling molecules and epigenetic factors. It is well-established

that Indian Hedgehog accelerates chondrocyte differentiation, balanced by FGF23 which retards chondrocyte differentiation, and parathyroid hormone-related peptide (PTHRP), that maintains the proliferation rate of chondrocytes (J. Guo et al., 2002; Kobayashi et al., 2002; Kronenberg, 2003). On the other hand, transcription factors such as Runx2 stimulate hypertrophic chondrocyte maturation and contribute to chondrocyte differentiation (Ducy et al., 1997; Enomoto-Iwamoto et al., 2001; Leboy et al., 2001; Otto et al., 1997). Further, Wnt/β-catenin signaling is required for normal cartilage and bone formation (Day et al., 2005).

2.2 Role of Phosphates in Regulating chondrocyte fate

The role of phosphates in cartilage mineralization is well-known. Optimal phosphate concentration is necessary to maintain sufficient circulatory levels and in the initial formation of hydroxyapatite crystals. Classically, whereas phosphate homeostasis is known to be controlled by parathyroid hormone and vitamin D by regulating intestinal absorption of phosphate and its reabsorption in the kidneys (Schiavi & Kumar, 2004), FGF23, which is mainly produced by osteocytes in bone, is a phosphaturic hormone. FGF23 is present in many tissues like liver, thymus, parathyroid, bone and heart (Shimada et al., 2001; Yamashita et al., 2000) and regulates phosphate metabolism by inhibiting Na-II pi co-transporter activity (Saito et al., 2003), thereby contributing to phosphate balance in the body. Thus, bone appears to function as an ‘endocrine organ’ via a complex bone-kidney axis.

DMP1 is a non-collagenous phosphoprotein of the SIBLING family (Fisher LW, 2003), a deficiency/mutation that leads to cartilage defects in mice and Autosomal Recessive Hypophosphatemic Rickets [ARHR] in humans (Ye et al., 2005), the latter being associated with increased levels of FGF23, thereby resulting in renal phosphate wasting (Feng et al., 2006). Mutations in (PHEX) phosphate regulating gene with homologies to endopeptidases on the X chromosome have also been associated with X-linked hypophosphatemia (Liu et al., 2008; Makras et al., 2008; Sabbagh et al., 2005; Yuan et al., 2008). Both these conditions occur through a common pathway of decreased phosphate levels in blood secondary to increased FGF23 levels. Further, FGF23 mutations are known to cause ARHR (Liu et al., 2008) by decreasing the number of proliferating chondrocytes and increasing their differentiation to hypertrophic chondrocytes, thereby causing achondroplasia (Colvin et al., 1996; Deng et al., 1996). Regardless, all the three mutations exhibit low phosphate levels in circulation, cause defects in cartilage and bone, and expanded growth plates with decreased apoptosis of the hypertrophic chondrocyte zone (Sabbagh et al., 2005).

Previous studies conducted in rachitic rats showed that phosphate is preferentially sequestered relative to calcium in the hypertrophic zone of the growth plate (Howell et al., 1968), and the size of inorganic phosphate crystals determines the degree of conversion of demineralized to mineralized cartilage (Bingham & Raisz, 1974; Kakuta et al., 1985). Studies on calcium-sensing receptor knockout mice have indicated that these mice exhibit hyperparathyroidism due to impaired calcium sensing, hypophosphatemia, and rachitic

changes despite hypercalcemia (Tu et al., 2003). All the above studies clearly indicate a correlation between low phosphate levels and rachitic changes in mice.

It is believed that decreased phosphate levels lead to decreased chondrogenesis, and decreased apoptotic rates in the hypertrophic chondrocyte layer. These effects result in the accumulation of hypertrophic chondrocytes, causing a further decrease in bone formation and maturation: such effects essentially attributable to defective chondrogenesis. By contrast, the proliferation layer of chondrocytes is wider (Lin et al., 2014). In addition, the bone in the subchondral regions and cortical compartments of long bones in DMP1-knockout (KO) mice is immature with high alkaline phosphatase activity (Feng et al., 2006). To date, no study has been able to offer a convincing explanation for the presence of an expanded hypertrophic chondrocyte layer, and the accumulation of poorly mineralized bone, in DMP1 KO mice. Hence, further elucidation is warranted.

2.3 Aims and Objectives

In this study, cell-lineage tracing techniques will be combined with multiple cellular and molecular approaches, to test the central hypothesis: 1) Low phosphate levels inhibits chondrogenesis and cell transformation from chondrocytes into bone cells; and 2) Low phosphate levels inhibits bone cell maturation.

Specific Aim 1 - Define chondrocyte fate in DMP1 KO mice (Hypophosphatemia model) using cell-lineage tracing techniques and other approaches.

Conventional DMP1 null mice that also harbor Aggrecan-Cre^{ERT2} and Rosa26^{tdTomato} will be used. In this way, the fate of chondrocytes in the DMP1 null mice can be traced after activating the cre event. Other approaches include digital radiography, μCT, Immunohistochemistry, Toluidine blue/ TRAP/ Alkaline Phosphatase Staining, and confocal microscopy to detect co-localization of COL1/ COL2/ COL10/ ENDOMUICN/ OSTERIX/ EDU/ OSTEOPONTIN/ KI67/RUNX2

Specific Aim 2 - To define the impact of Pi levels (low and high Pi) on secondary ossification formation using the metatarsal organ culture model.

For this, 10-day old metatarsal rudiments will be harvested from DMP1 null mice and DMP1 control mice and cultured at varying phosphate concentrations; concentration-dependent effects on the formation of secondary ossification centers will be looked for using digital radiography.

2.4 Rationale

It is hypothesized that decreased phosphate levels inhibit chondrogenesis; using cell-lineage tracing, the chondrocyte cell line can be traced from the resting zone to the hypertrophic zone (until bone formation) of the growth plate, after which it should be assessible whether the observed phenotype (in Aggrecan-Cre to DMP1 null mice) is due to a defect in endochondral ossification, or intramembranous ossification; any defect or delay in the cell transformation to bone cells will be traced.

The above-mentioned cell line combined with in vitro approaches will be used to test the hypothesis.

CHAPTER III

MATERIAL AND METHODS

3.1 Development of Mice

The fate of the post-natal chondrocytes in subchondral bone formation and its relationship to phosphate was studied by generating triple mice lines using the following strains Agg-Cre^{ERT2} (Henry et al., 2009; G. Yang et al., 2005), DMP1$^{-/-}$, and Rosa26^{tdTomato} (B6;129S6-Gt(ROSA)26Sortm9(CAG-tdTomato)Hze/J, stock number: 009705; Jackson Laboratory, Bar Harbor, ME, USA) as described previously (Jing et al., 2015), (Soriano, 1999) and internally cross breeding the mice lines thrice. Dmp1$^{-/-}$ mice with exon 6 deletion were generated as described previously.(Feng et al., 2006). All the animals(mice) that were used for this study were maintained under the guidelines established by the Institution of Animal Care and Use Committee (IACUC, Texas A&M University College of Dentistry), which carry out required approval for all the procedures used in this study. All the pups were induced once with Tamoxifen at P3 (7.5µl /1 gm of body weight) and sacrificed at 10 days of age. Tamoxifen (T5648; Sigma-Aldrich, St. Louis, MO, USA) was dissolved in 10% ethanol and 90% corn oil (C8267; Sigma-Aldrich) as described previously (Jing et al., 2015). 4 mice were used in each group for each specific aim, along with controls which contain DMP1 (DMP1$^{+/+}$). All the mice lines were generated in a C57BL/6 background. The mice were fed with autoclaved Purina rodent chow (5010; Ralston Purina, St Louis, MO, USA) containing calcium, 0.67% phosphorus, and 4.4 IU of vitamin

D per gram. For observing the cell proliferation rate, 5–ethynyl–2′–deoxy uridine (EDU) was injected [at 3ml/gm of body wt.] 24 hours before sacrifice.

3.2 Digital Radiography (X-Ray) and Micro-Computed Tomography

The skeletons of DMP1 mice and DMP1-null mice were examined using digital radiography (Faxitron MX-20DC12 system; Faxitron Bioptics, Lincolnshire, IL, USA) at 10 days after fixation in 4% paraformaldehyde (PFA) for 24 hours, followed by fixation in 0.5% PFA. The tibias were scanned in a μ-CT imaging system (35, Scanco Medical, Bassersdorf, Switzerland) as described previously (Ye et al., 2005). Tibia cortical bone and whole bone data were quantified using a μCT imaging system. Serial tomographic imaging at an intensity of 145 μA and energy level 55Kv for the tibia was done. For this purpose, cortical bone from 120 cross-sectional slices above the mid-shaft of the tibia was analyzed. The threshold used for this analysis was 200. Bone volume/total volume [BMD] at the mid-shaft was also calculated and used for comparison between the samples. The porosity, and apparent and material densities were also obtained. For calculating the trabecular bone volume, a total of 183 slices below the growth plate area and above the mid shaft area was analyzed. The porosity, apparent and material densities, and bone volume/total volume [BMD] was obtained, calculated and used for comparison between the samples.

3.3 Histology

Toluidine Blue Staining

To prepare frozen sections, the specimens were first fixed in 4% PFA in PBS (at pH 7.4) for 24 hours, then transferred to 0.5% PFA in PBS (at pH 7.4). Further decalcification of specimen in 17% EDTA was done. Then, the samples were immersed in 30% sucrose overnight, later embedded in OCT and left for 30 minutes to freeze up in the cryostat. Finally, the samples were sectioned into 10µm sections. The sections were dried for 40 minutes at room temperature and later stored at – 20 ^{o}C, pending staining or immunofluorescence, or till other procedures were done.

For any staining procedures, the sections were incubated in 37 ^{o}C for 10 minutes, then at room temperature for another 2-3 minutes, washed with distilled water twice for 5 minutes at room temperature to hydrate the slides and to remove OCT. After washing, the slides were stained in toluidine blue working solution for 5 minutes and once again washed in distilled water till clear. After staining, a series of dehydration steps were followed: first dipping the slides in 80% alcohol for 30 seconds, then air dried; a second dip in 100% alcohol twice for 3 minutes, then air dried; a final dip in Xylene twice for 2 minutes, then air dried; the slides were then cover-slipped with permount and left to dry overnight, before being observed under microscope.

TRAP Staining

After the slides were hydrated and the OCT removed, 2 Coplin jars A & B containing 40 ml of trap buffer 1 [(Sodium acetate anhydrous (sigma S-2889) – 9.2 gm, L tartaric acid (sigma T-6521) – 11.4 gm, distilled water – 950ml, glacial acetic acid (sigma 320099), with PH adjusted to between 4.7-5.0 using 5M sodium hydroxide] were incubated at 37 ^{o}C for 15-20 minutes; then buffer II [Naphthol AS-BI phosphate (sigma N-2125) – 20 mg & Ethylene glycol monoethyl ether (sigma E-2612) – 1ml] is added to jar A and the slides are immersed into the jar and incubated for 45 minutes with the Jar B still remaining in the incubator for an additional 45 minutes along with Jar A. Then, just before 45 minutes lapsed, Buffer III [sodium nitrite (sigma S-2252) – 40 mg, distilled water – 1ml] and Buffer IV [Parasoniline chloride (Basic Fuschin, Sigma P–3750) – 50 mg, distilled water – 834µl, Hcl – 166 µl] were prepared. Buffer IV was heated for 5 minutes at 55 ^{o}C and filtered. The two buffers were then mixed for 30 secs and allowed to stand still for 2 minutes. Later, this combined mixture was added to jar B and the slides from jar A are then transferred to Jar B immersed for 10 seconds and then washed in distilled water to stop the reaction; the slides were then observed under microscope. Finally, the slides were counterstained with methylene green for 5 minutes, washed with distilled water and the series of dehydration steps followed in the same way, as described for Toluidine Blue staining.

Alkaline Phosphatase Staining

Alkaline Phosphatase is an enzyme which determines the amount of osteoblastic activity (greater the staining intensity, more is the osteoblastic activity).

After the slides were brought to room temperature, they were washed with PBS for 5 minutes; the slides were first incubated in PBST at 37 ºC for 5 minutes, then incubated in ALP staining buffer for 10-30 minutes, depending on the staining intensity. After the slides were washed with PBS [to stop the staining reaction], they were observed under microscope; slide counter staining with methylene green for 5 minutes was done and the dehydration steps were followed, as described above. Finally, the slides were cover slipped, and allowed to dry overnight in preparation for imaging the next day.

3.4 Immunostaining and Immunofluorescence

Immunostaining was done with different primary and secondary fluorescent antibodies. The frozen slides were incubated at 37 ºC for 10 minutes, left at room temperature for 3 minutes, and then washed in distilled water twice for 5 minutes. After that they were incubated with IHC working solution at 37 ºC for 40 minutes, slides were washed with PBS, 3 times, for 3 minutes; then, for a polyclonal primary antibody, the blocking solution (prepared using 3% BSA, 20% goat serum and PBS) was added to slides, and incubated for 1 hour at room temperature. Then, the blocking solution was removed carefully using blotting paper and the primary antibody was added according to the working range

concentration; the slides were then incubated at 4 ºC, overnight. On day 2, the slides were washed with PBS 3 times for 3 minutes, and the secondary antibody (in the concentration of 1:200, 4% goat serum, PBS) were used and the slides were incubated at room temperature for 2 hours, then washed with 1% PBS 3 times for 3 minutes; the slides were mounted using DAPI mounting medium and allowed to dry. For immunolocalization, the following antibodies were used: anti-col1 rabbit polyclonal antibody (1:100; Abcam, Cambridge, England), anti-Col2 mouse monoclonal antibody (1:50; Santa Cruz Biotechnology, Dallas, TX, USA), anti-Col10 rabbit polyclonal antibody (1:100; provided by Dr. Natasha Cherman from NIH)), anti-SOST antibody (1:100; R&D systems), anti- KI67 antibody (1:100 Thermo Fischer Laboratories, USA), anti- Runx2 antibody(1:400; cell signaling technologies, USA), anti- Osterix antibody (1:400 Abcam ; USA), anti- Endomucin antibody (1:100 Abcam ; USA)

3.5 Confocal Microscopy

All fluorescent cell images were captured at wavelengths ranging from 488 (green) – 561 (red) nm, using an SP5 Leica Confocal Microscope. Multiple, stacked images were taken at 200Hz (1024 x 1024) and the different chondrocyte zones [and their contribution to subchondral bone formation] were observed.

3.6 In vitro (Metatarsal) Organ Culture

For culture, the three central metatarsal bone rudiments were dissected out from the hind limbs of 10-day old DMP1 null mice and their age-matched control litter mates and

cultured in a 24-well plate [one bone per well], as described previously (R. Zhang et al., 2011).

3.7 Statistical Analysis

As the groups were homogenous, a total number of 3 samples for each group were considered; a student ‘t’ test was carried out for two-group comparisons and a p value of < 0.05 was considered statistically significant.

CHAPTER IV

RESULTS

Dmp1 KO mice display significant bone defects

By using radiographs examination, we observed a significant delayed secondary ossification in epiphysis with more metaphyseal bone and dramatic reduction of limb length in P10 KO mice (Fig. 8 , right panel). Toluidine Blue Staining showed increased cartilage residue and more metaphyseal bone in the bone matrix (purple color – Fig 9, right panel) in 10-day old KO mice. Furthermore, (ALP) staining displayed expanded hypertrophic chondrocyte layers and highly active in cell differentiation from hypertrophic chondrocytes to osteoblasts (dark blue color--Fig 10a, right panel) in KO mice at P10. Since there is active chondrocyte cell proliferation in the growth plate area and more bone in the metaphysis area, TRAP activity was examined to find if there is an equal rate of osteoclastic resorption too. Trap staining revelaed that there is no difference in TRAP activity between control and KO when compared in unit bone surface area (Figure 10b, left and rightpanel). All the histological studies revelaed that the entire chondrogenesis is accelerated with active differentiation in KO mice.

Cell Lineage Tracing

Cell lineage tracing technique was used to investigate the mechanism for the dramatic increase of bone volume in the diaphysis and metaphysis but significant delay in

secondary ossfication and bone growth in KO mice. First DMP1 conventional knockout mice were generated (Feng et al., 2006). In order to trace the cell fate, the DMP1 KO mice were crossed with the Aggcrecan-Cre^{ERT2} (expressed in all cartilage cells) with $R26R^{Tomato}$ mice. In this way, all the chondrocytes and their descendents were labelled with a red color after the Cre event is activated by one-time tamoxifen injection. cell lineage tracing was combined with immunostaining for different proteins.

First, osteogenic related proteins were used to examine the difference in bone formation between DMP1 KO and control mice. Collagen 1 (COL1) forms most of the organic component of bone. COL1 expression was reduced in the epiphysis and at the articular surface in KO mice, which may imply that cell transformation is affected because COL1 forms most of the organic component of bone and its reduction signifies that the cells are still in the chondrogenesis phase. (Fig 11a, right panel). As expected, more COL1 expression was seen in the metaphysis, indicating more bone matrix in the KO mice (Fig 11b, right panel). Next the expression of OPN, a glycoprotein which also forms the organic component of bone was studied. Like COL1, it is decreased in epiphysis area in KO mice (Fig 12a, right panel) and increased dramatically in bone matrix in metaphysis (Fig 12b, right panel).

Next, transcription factors Runx2 and OSX were examined. Runx2 is a critical transcriptional factor for osteoblast differentiation. Osx is also an important transcriptional factor necessary for osteoblast activation. The expression for both was decreased in

epiphysis and metaphysis in the 10-day old KO mice (Runx2-Fig 13a, 13b, right panel), (OSX - Fig 14a, 14b, right panel). Then proliferation markers KI67, EDU were used to examine proliferative activity of cells right from induction of cre and the 24-hour proliferative activity of cells (EDU). Ki67 activity was higher in proliferative, prehypertrophic, hypertrophic chondrocytes (Fig 15a, right panel) and in bone (Fig 15b, right panel). This demonstrates that there is active cell division taking place, contributing to more chondrocyte cell numbers and bone cells in KO mice. However, EDU activity was the same in control in epiphysis (Fig 16a, left panel) and metaphysis (Fig 16b, left panel). Early cartilage marker (COL2) which is expressed by all cartilage cells & late cartilage marker (COL10) which is specifically expressed by only hypertrophic chondrocytes was then examined. We found that the COL2 is similar in both epiphysis (Fig 17a, left and right panel) and in bone matrix (Fig 17b, left and right panel) when compared in unit surface area in control & KO mice. COL10 expression is higher in control in epiphysis (Fig 18a, left panel) and in bone matrix (Fig 18b, left panel). Lastly, osteocyte marker sclerostin (SOST) and endothelial Marker Endomucin were used to examine the cell maturation and vascularity. SOST expression is higher in control mice both in epiphysis (Fig 19a, left panel) and in cortical bone in diaphysis area (Fig 19b, left panel). Endothelial marker Endomucin expression is higher in epiphysis of control mice (Fig 20a, left panel). But the Endomucin activity is relatively similar in control and KO mice (Fig 20b, left and right panel) in unit square surface area.

Micro CT Analysis

Micro – CT analysis was performed to determine the quality of bone formed in metaphysis. The structural cortical bone data revealed that there is more cortical bone and trabecular bone in KO mice (Fig21, right panel) however the bone appears more porous. Material density is the actual density of bone excluding the pores and Apparent density of the material is the density of bone including the pores. Quantitative analysis revealed that there was less material density for cortical (Fig 22) and trabecular bone (Fig 23) in KO mice. There was no significant difference in Apparent density in cortical bone between control and KO mice suggesting that the cortical bone formed is of relatively good quality in KO (Fig 24). However, the Apparent density of trabecular bone is significantly high in KO (Fig 25). Trabecular number is higher in KO mice which was expected due to more trabecular bone (Fig 26). Trabecular separation was less in KO mice which was expected because of more compacted trabecular bone in metaphyseal area (Fig 27). Cortical BV/TV is reduced in KO mice suggesting that though the bone appears dense, it is porous and therefore its bone volume is reduced (Fig 28). Trabecular BV/TV was high in KO mice which was expected due to more trabecular bone volume (Fig 29).

Ex Vivo Metatarsal Organ Culture

To investigate the role of phosphate on cell transformation and cell maturation independent of systemic factors, metatarsal organ culture studies were done for 8 days on P10 control and KO mice. This revealed that with increased β Glycero phosphate

concentration from 0 milli molar to 3 milli molar concentration, the secondary ossification center begins to form in KO mice like control mice (Fig 31) suggesting that phosphate plays a significant role in cell transformation and cell maturation. Lastly radiographs of KO mice revealed that the caudal vertebrae are smaller in size than control mice (Fig 30) and the reasons for this phenotypic change will be explored further.

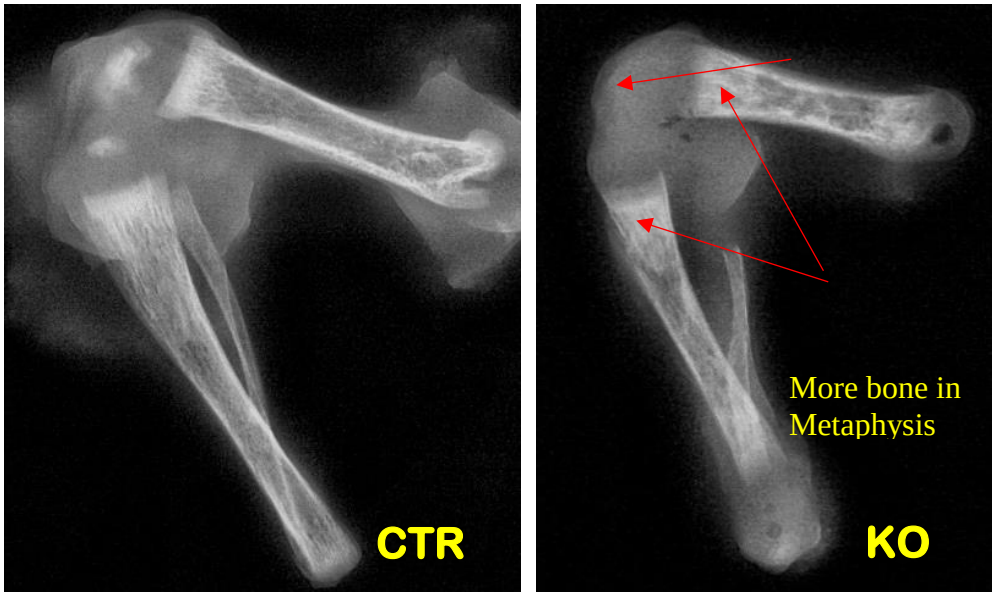

Figure 8. Delayed Secondary Ossification: Representative X -ray images showed delayed secondary ossification and more metaphyseal bone in P10 KO mice (red arrow).

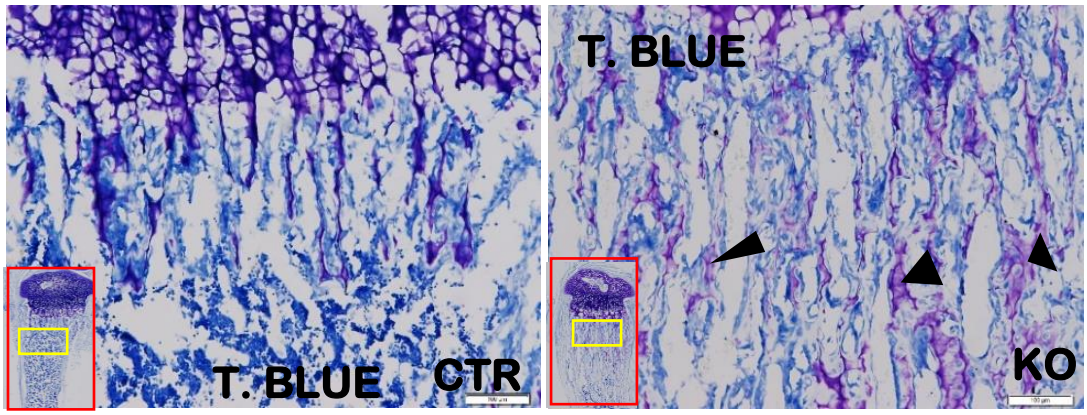

Figure 9. Toluidine Blue Staining: Representative Toluidine Blue images showed increased cartilage residue (purple) and more bone mass in metaphysis area in KO mice (black arrow heads)

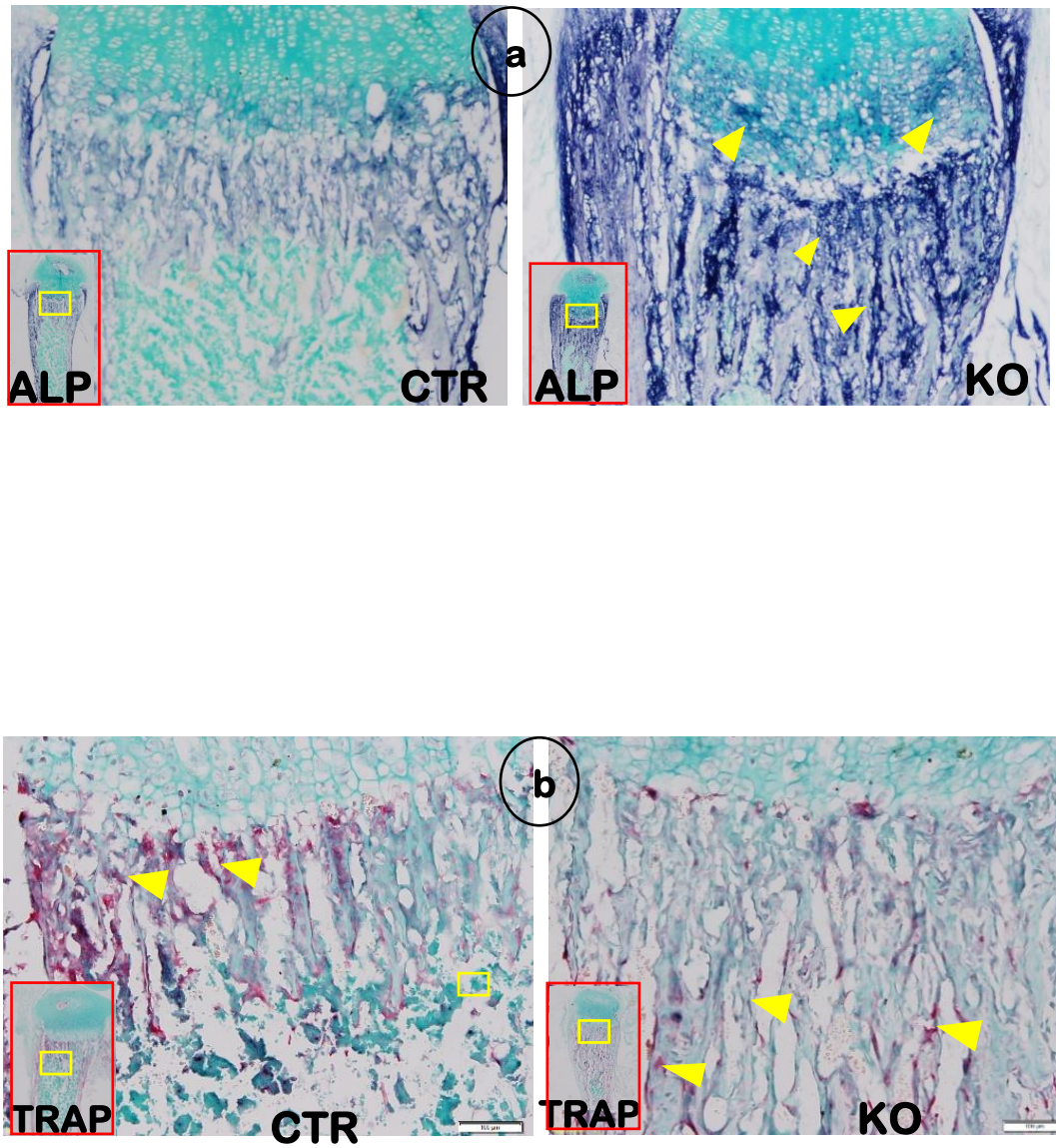

Figure 10. a. ALP Staining: Representative Alkaline Phosphatase (ALP) stain images showed increased ALP activity (blue stain) in hypertrophic chondrocytes and metaphysis bone area in KO mice (yellow arrow heads). **Figure 10.b. TRAP Staining:** Tartarate – resistant acid phosphatase (TRAP) stain images show similar osteoclastic activity (red stain) in both control and KO per unit bone surface area (yellow arrow heads).

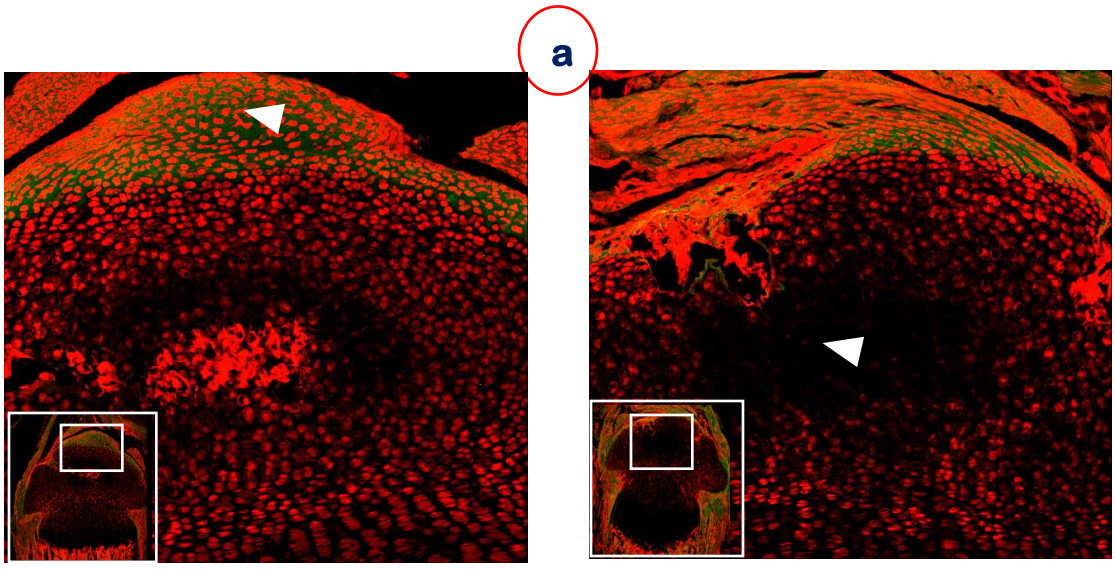

Figure 11a. Immunostaining COL1 in epiphysis: COL 1 Immunostaining (green) co-localized with cell lineage tracing by using Aggrecan-CreERT2 (red) showed decreased COL1 activity in articular surface and delayed secondary ossification (white arrow heads) in **epiphysis** in KO mice.

.

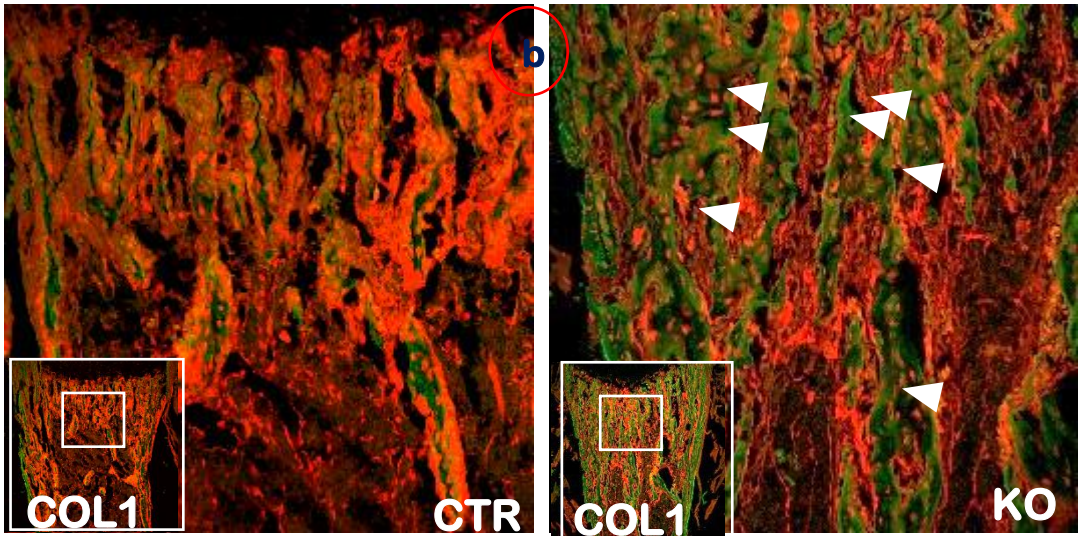

Figure 11b. Immunostaining COL1 in bone matrix: COL 1 immunostaining images showed more COL1 activity in bone matrix (white arrow heads) in metaphysis in KO mice.

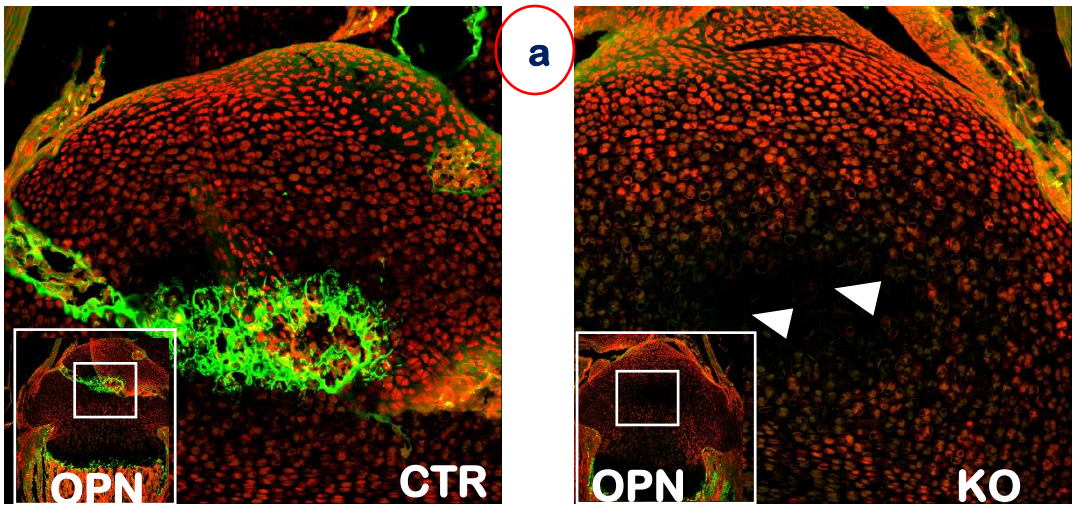

Figure 12a. Immunostaining OPN in epiphysis: Osteopontin (OPN) immunostaining (green) co-localized with cell lineage tracing by using *Aggrecan-Cre*^{ERT2} (red) showed decreased OPN activity and delayed secondary ossification (white arrow heads) in epiphysis in KO mice.

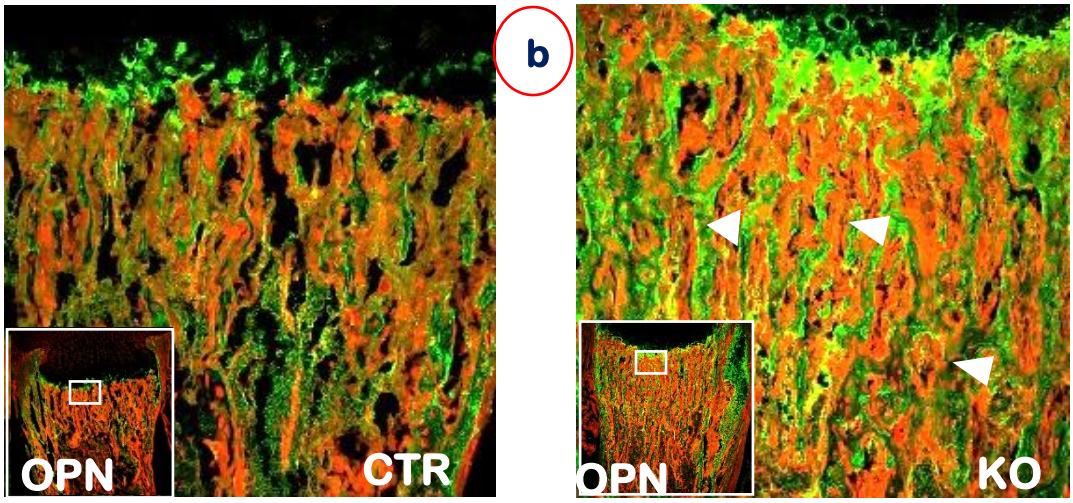

Figure 12b. Immunostaining OPN in bone matrix: Osteopontin (OPN) immunostaining images showed increased OPN activity in bone matrix in KO mice (white arrow heads).

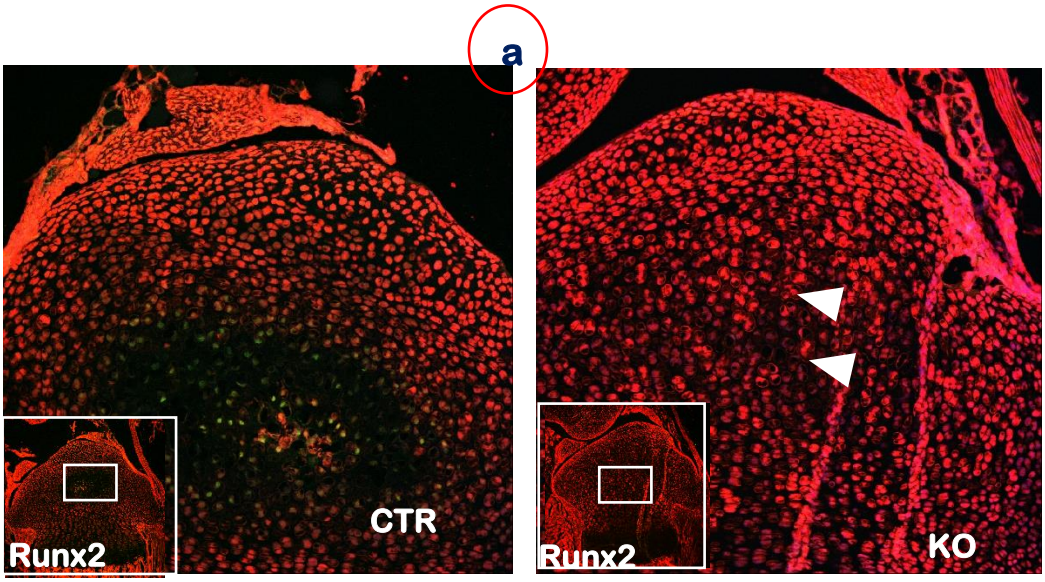

Figure 13a. Immunostaining Runx2 in epiphysis: Runt related transcription factor (Runx2) immunostaining (green) co-localized with cell lineage tracing by using *Aggrecan-Cre*^{ERT2} (red) and Dapi (blue) showed no Runx2 activity in articular surface and increased chondrogenesis (white arrow heads) in epiphysis in KO mice

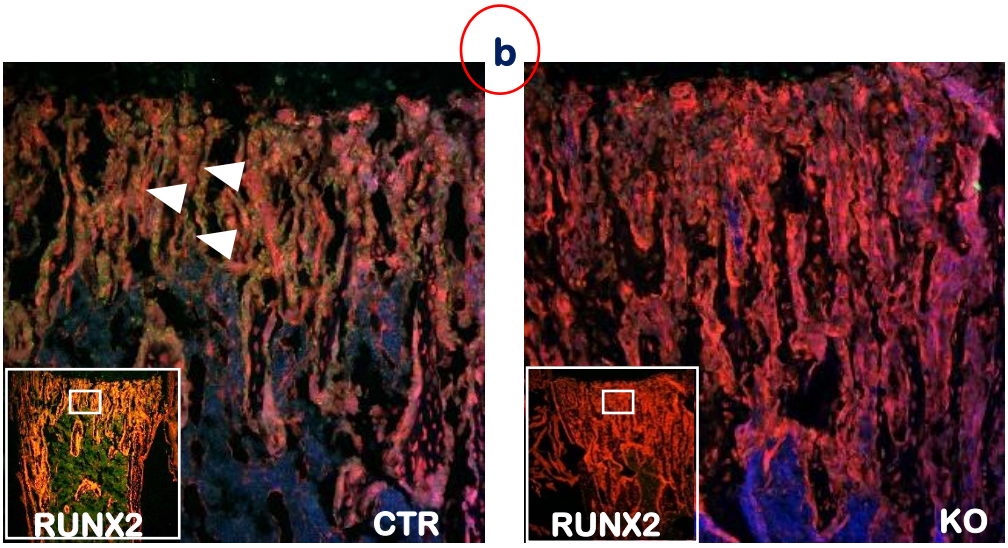

Figure 13b. Immunostaining Runx2 in bone: Runt related transcription factor (Runx2) immunostaining showed increased Runx2 activity in control in bone matrix (osteoblasts) than KO (white arrow heads).

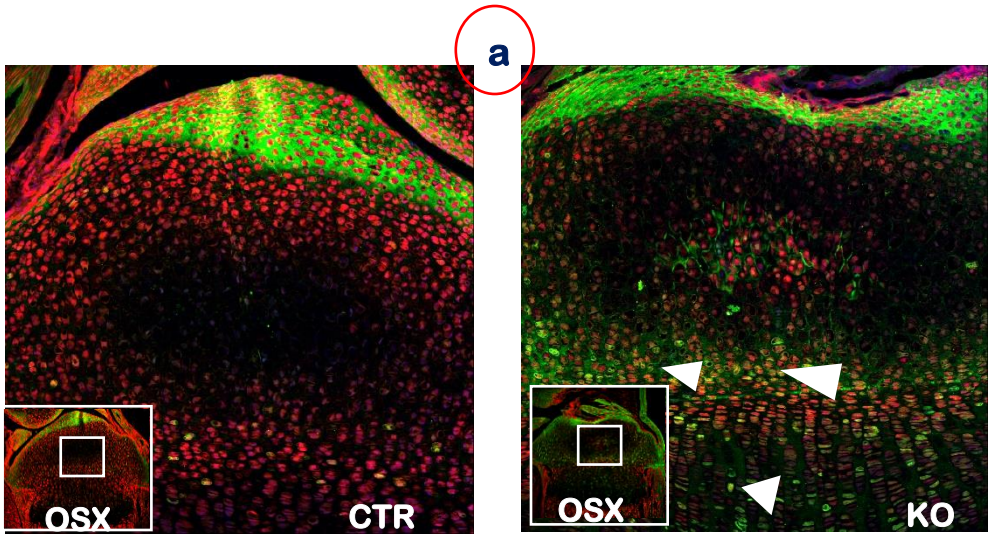

Figure 14a. Immunostaining OSX in epiphysis: Osterix (OSX) immunostaining (green) co-localized with cell lineage tracing by using *Aggrecan-Cre*^{ERT2} (red) and Dapi (blue) showed more Osx activity (osteoblast) in proliferative and prehypertrophic chondrocytes (white arrow heads) in epiphysis in KO mice.

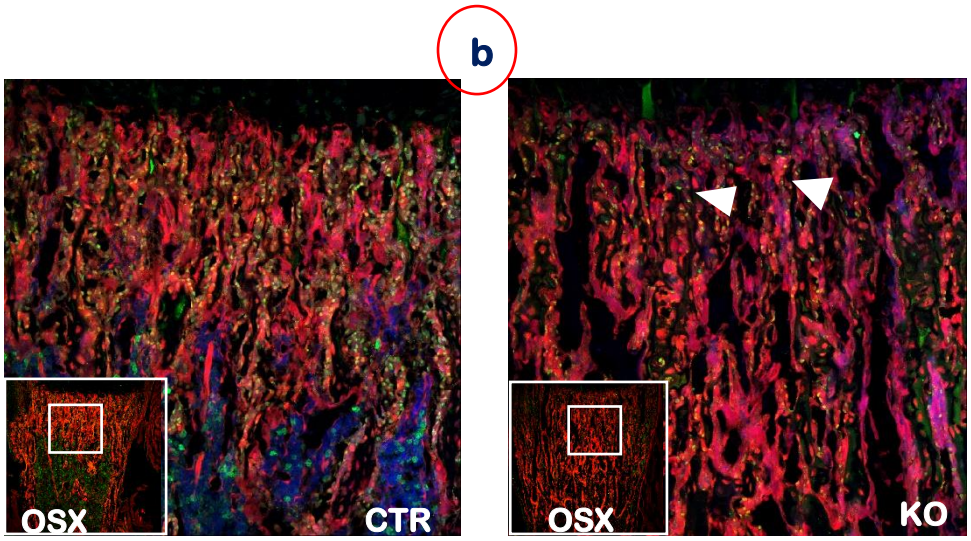

Figure 14b. Immunostaining OSX in bone: Osterix (OSX) immunostaining images showed less Osx activity (osteoblast) in bone cells (white arrow heads) in KO mice.

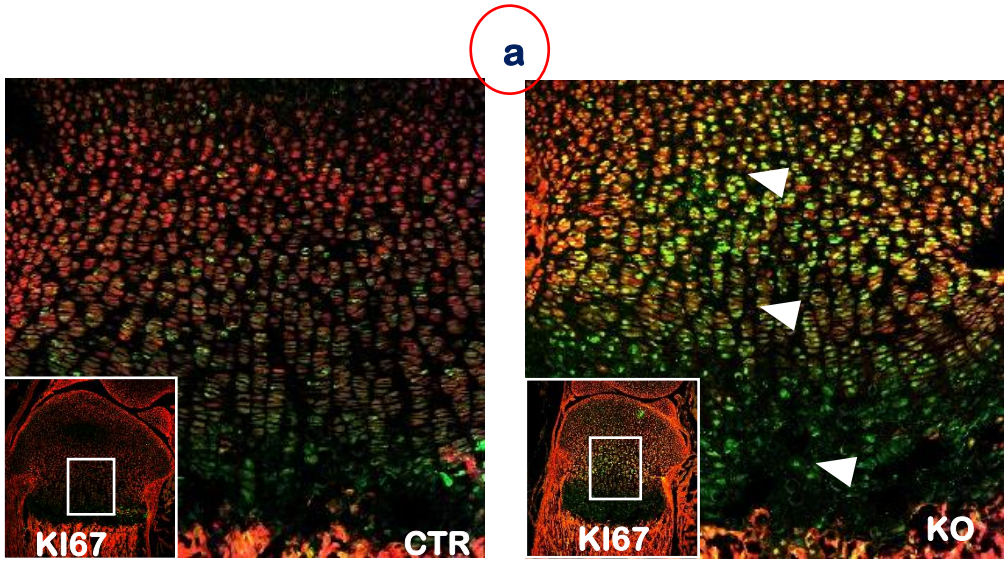

Figure 15a. Immunostaining KI67 in epiphysis: Ki67 immunostaining (green) co-localized with cell lineage tracing by using *Aggrecan-Cre*^{ERT2} (red) and Dapi (blue) showed increased proliferative (KI67) activity in proliferative and pre-hypertrophic/ hypertrophic chondrocytes in epiphysis KO mice (white arrow heads) at P10.

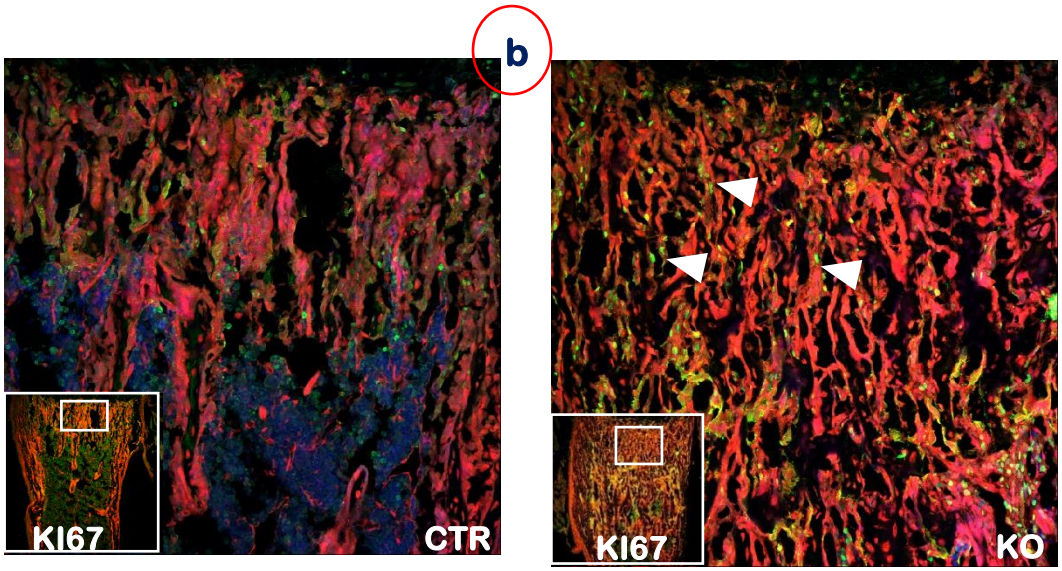

Figure 15b. Immunostaining KI67 in bone: KI67 immunostaining images showed increased proliferative (KI67) activity of osteogenic cells on the bone surface in KO mice (white arrow heads).

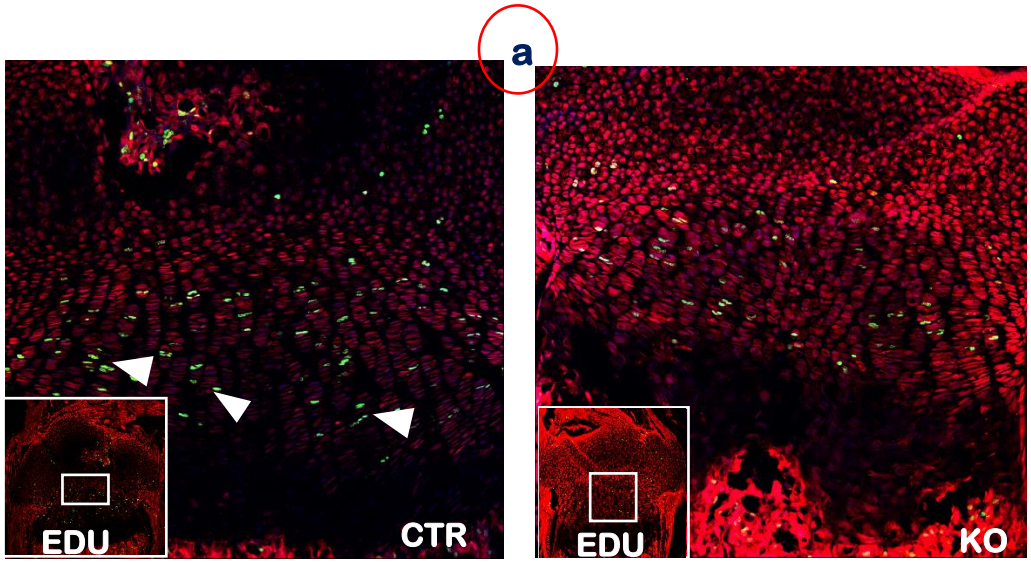

Figure 16a. Immunostaining EDU in epiphysis: EDU immunostaining (green) co-localized with cell lineage tracing by using *Aggrecan-Cre*^{ERT2} (red) and Dapi (blue) showed increased proliferative (EDU) activity in epiphysis in proliferative and pre-hypertrophic in control mice (white arrow heads).

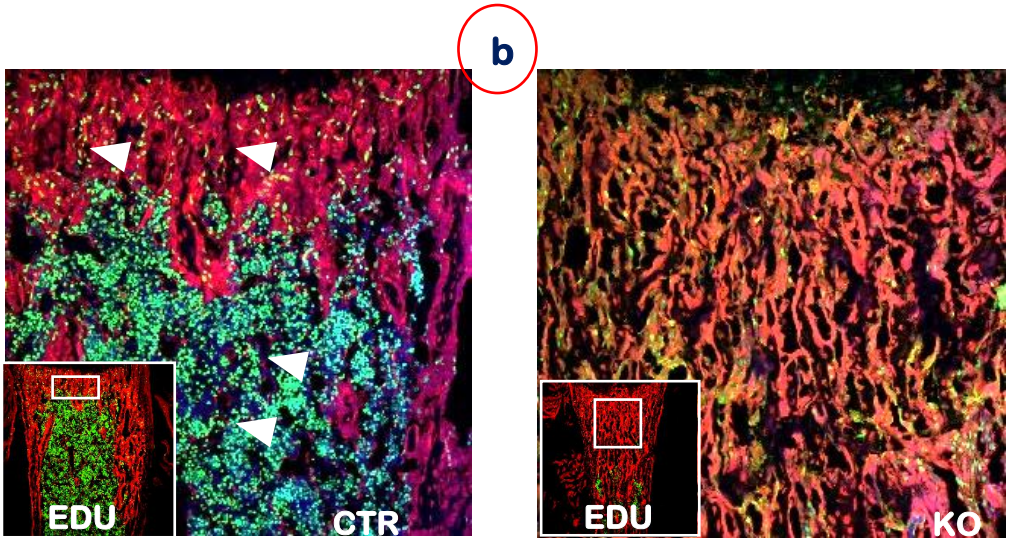

Figure 16b. Immunostaining EDU in bone: EDU positive cells in bone marrow and the osteogenic cells on the **bone** surface in metaphysis in 10-day old control mice were much more than the KO mice.
(white arrow heads).

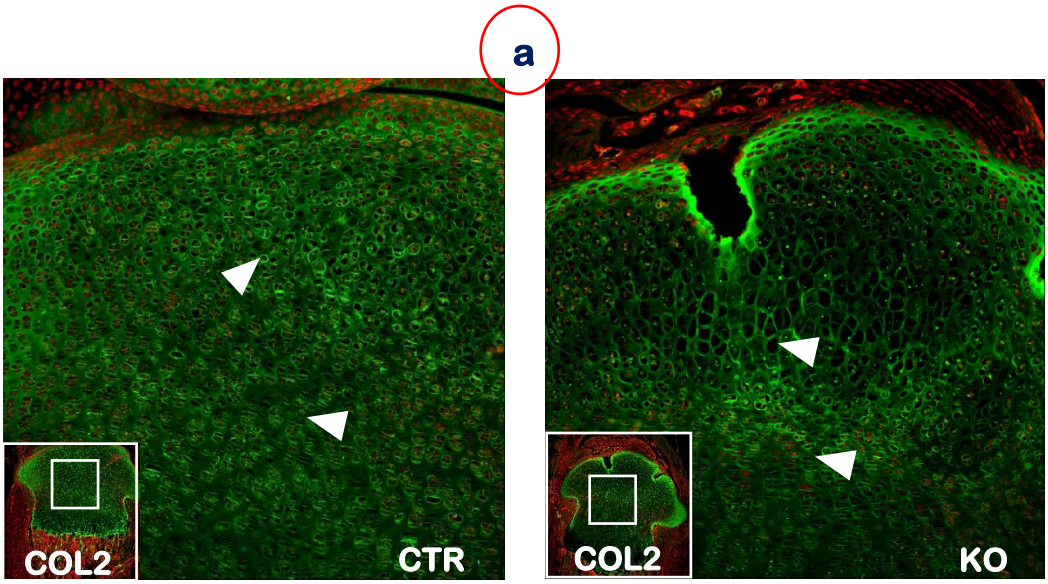

Figure 17a. Immunostaining Col2 in epiphysis: collagen 2 (COL2) immunostaining (green) co-localized with cell lineage tracing by using *Aggrecan-Cre*^{ERT2} (red) showed similar COL2 activity in both control and KO mice at P10 in epiphysis and proliferative chondrocytes (white arrow heads).

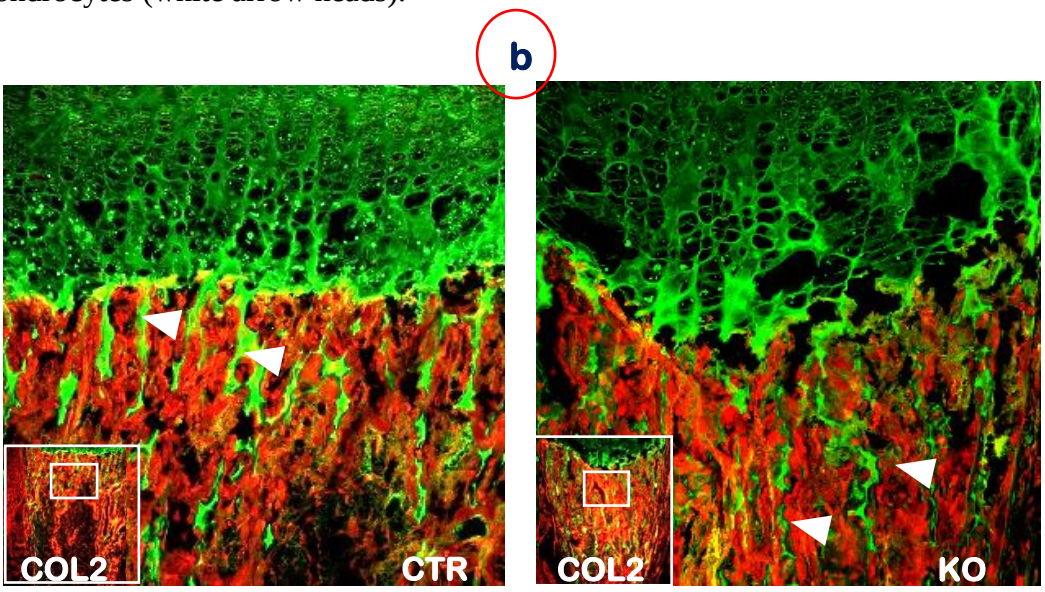

Figure 17b. Immunostaining Col2 in bone: There was no significant difference in the cartilage residue reflected by COL2 immunostaining in metaphysis (bone matrix) both 10-day old control and KO mice (white arrow heads).

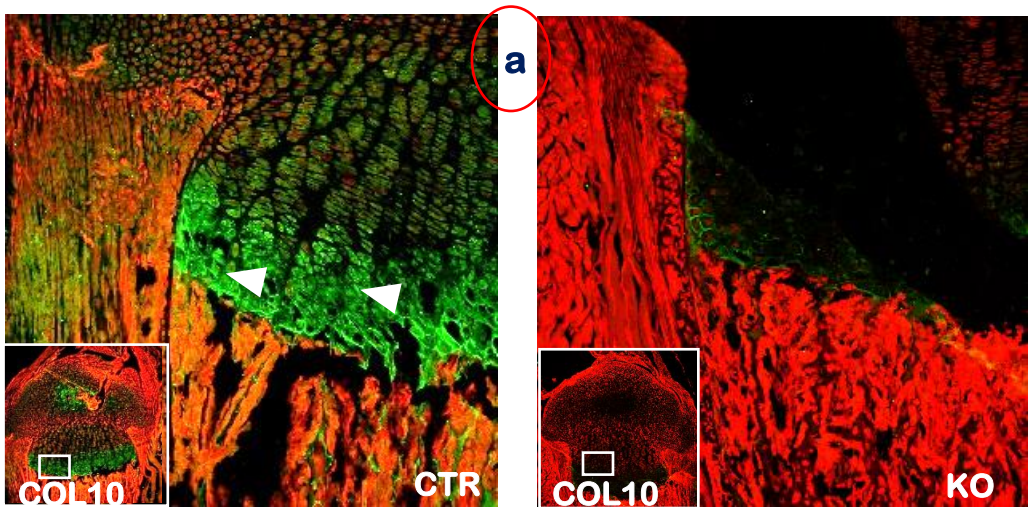

Figure 18a. Immunostaining Col10 in growth plate: Collagen 10 (COL10) immunostaining co-localized with cell lineage tracing by using *Aggrecan-Cre*^{ERT2} (red) showed a strong COL10 expression in the hypertrophic chondrocytes (white arrows heads) in the control growth plate, but an absence in the age-matched KO mice.

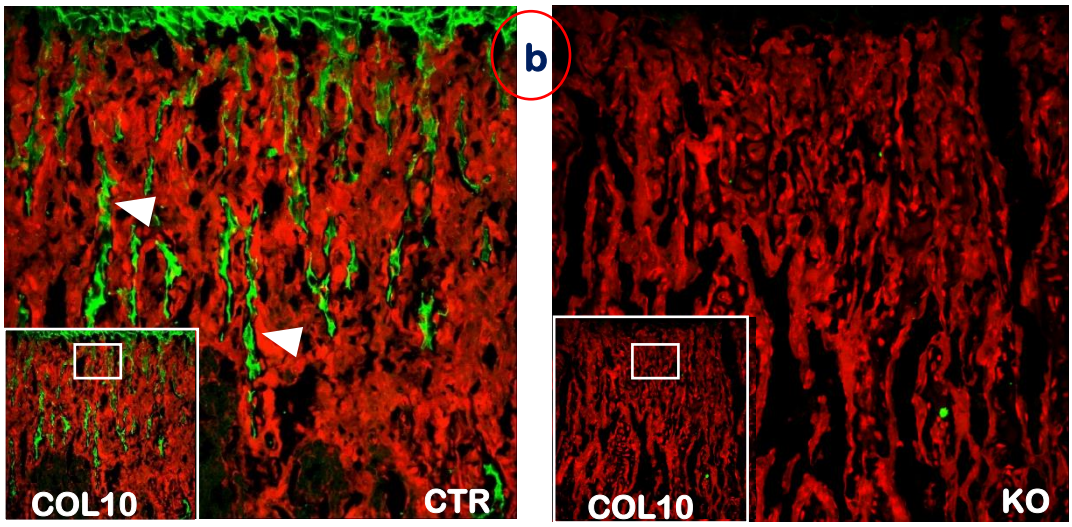

Figure 18b. Immunostaining Col10 in bone: COL10 expression was also higher in the metaphysis (bone matrix) in control compared with KO mice (white arrows heads).

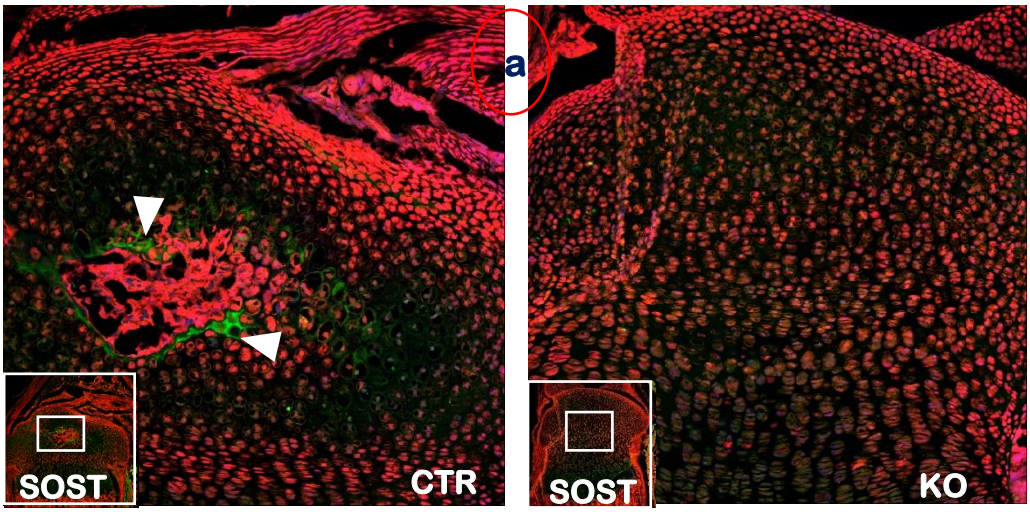

Figure 19a. Immunostaining SOST in epiphysis: Sclerostin (SOST) immunostaining (green) co-localized with cell lineage tracing by using *Aggrecan-Cre*^{ERT2} (red) and Dapi (blue) revealed a positive expression of Sclerostin in the secondary ossification in control mice, while there was no sign for an ossification in the epiphysis in the KO mice (white arrows heads).

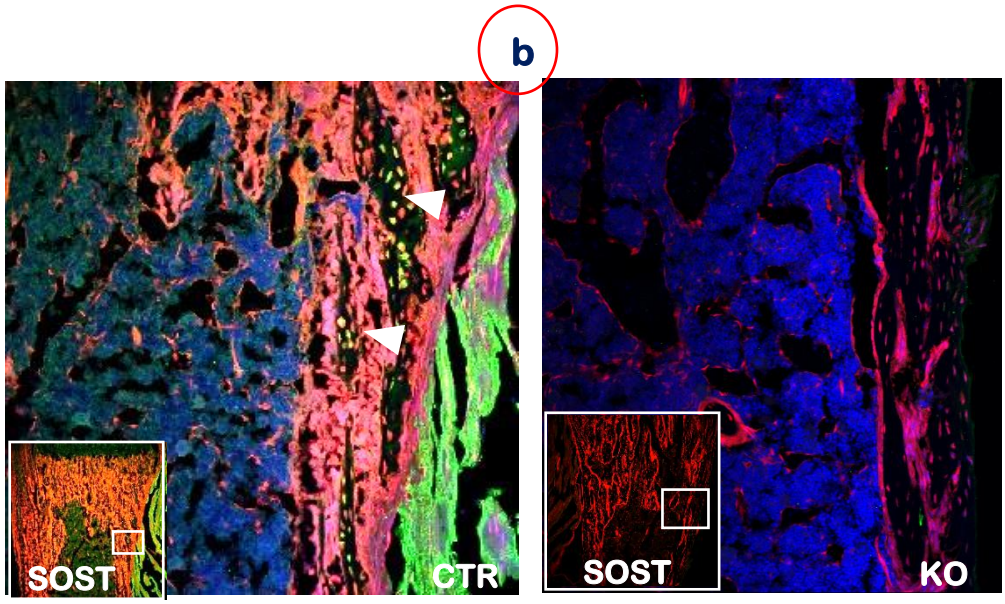

Figure 19b. Immunostaining SOST in bone: SOST was highly expressed by osteocytes in the osteocytes in the control cortical bone, but was barely detected in the KO mice (white arrows heads).

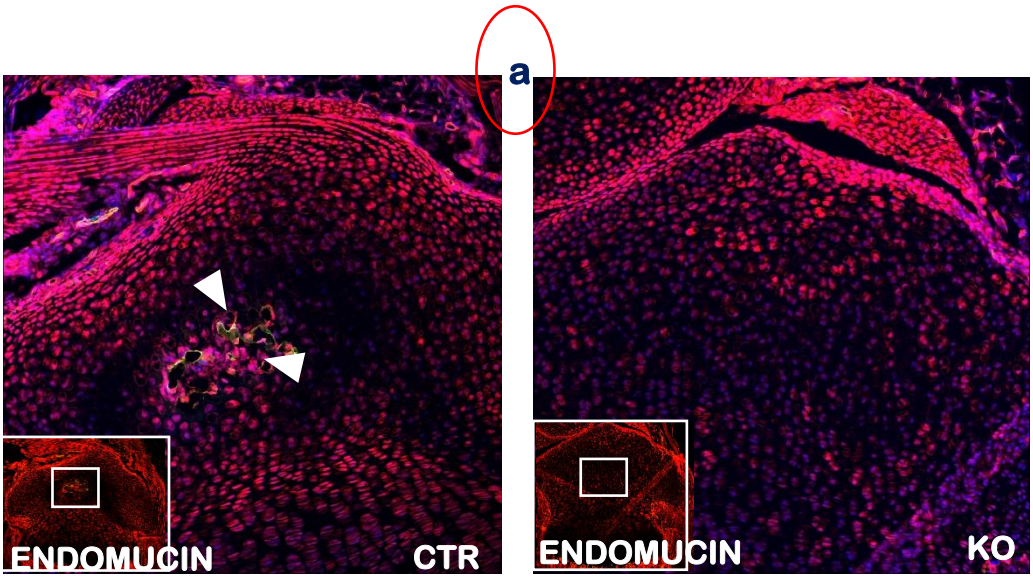

Figure 20a. Immunostaining Endomucin in epiphysis: Endomucin immunostaining (green) co-localized with cell lineage tracing by using *Aggrecan-Cre*^{ERT2} (red) and Dapi (blue) revealed a positive expression of Endomucin in the secondary ossification in control mice, while there was no sign of any vascularity in the epiphysis in the KO mice (white arrows heads).

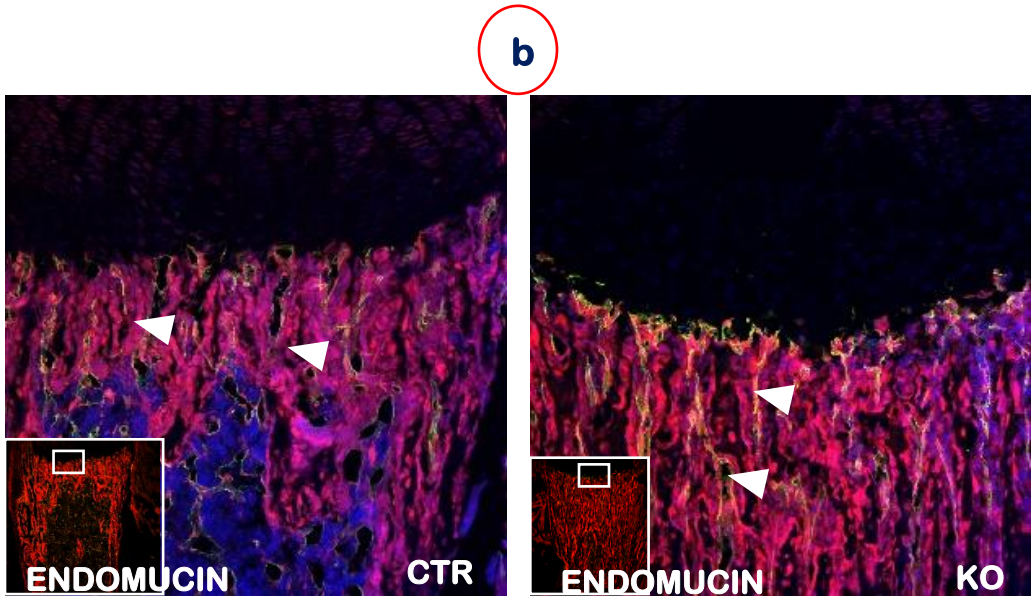

Figure 20b. Immunostaining Endomucin in bone: Endomucin immunostaining images showed similar Endomucin activity in both control and KO mice per unit bone surface area (white arrow heads).

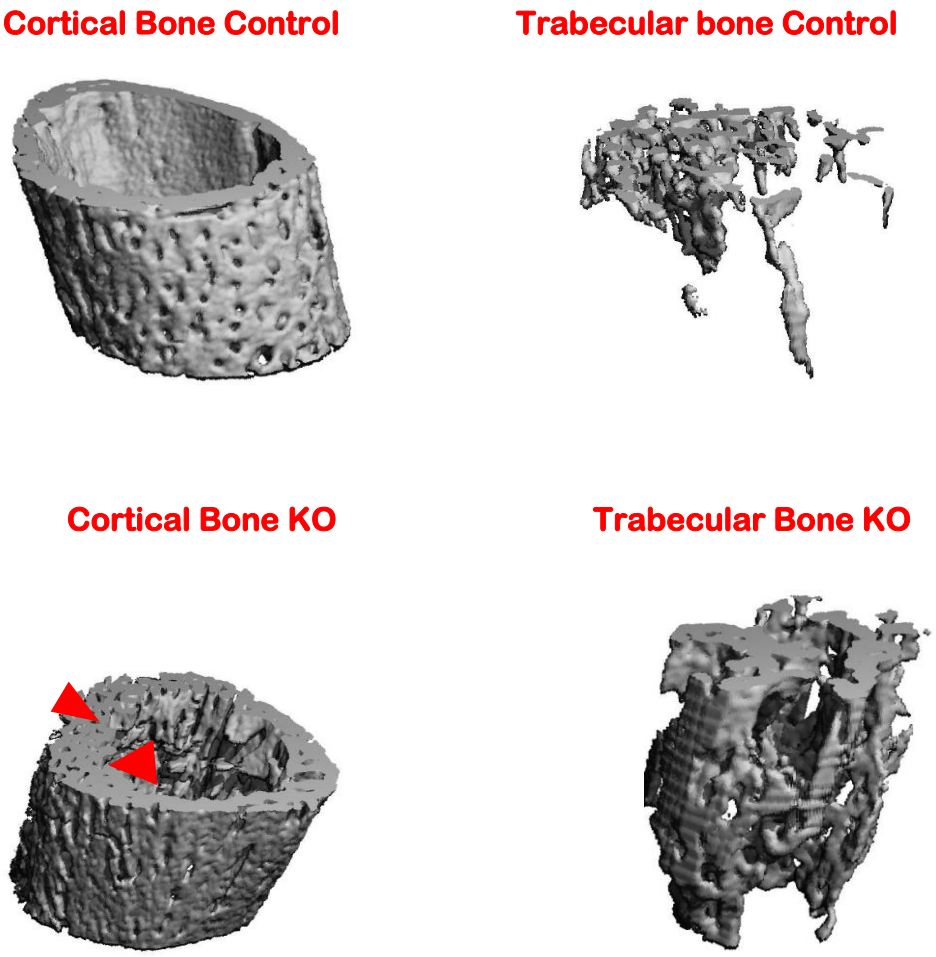

Figure 21. Micro CT Imaging Data: From the above micro – CT data, we can clearly observe that the overall cortical and trabecular bone volume seems to be more in KO than Control, although most of bone is porous in KO (red arrows) at P10.

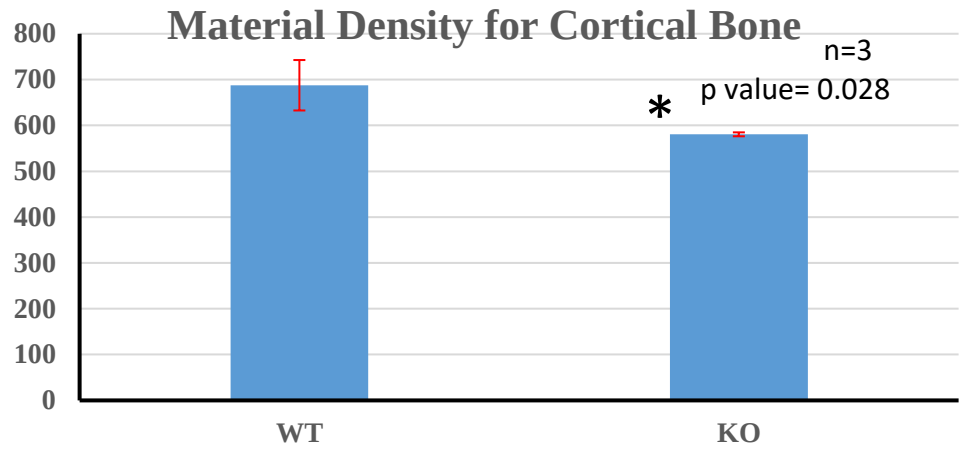

Figure 22. Material Density for Cortical Bone Graph: Quantitative analysis of Material density for cortical bone showed a statistically significant difference between control and KO samples (n=3, $P < 0.05$).

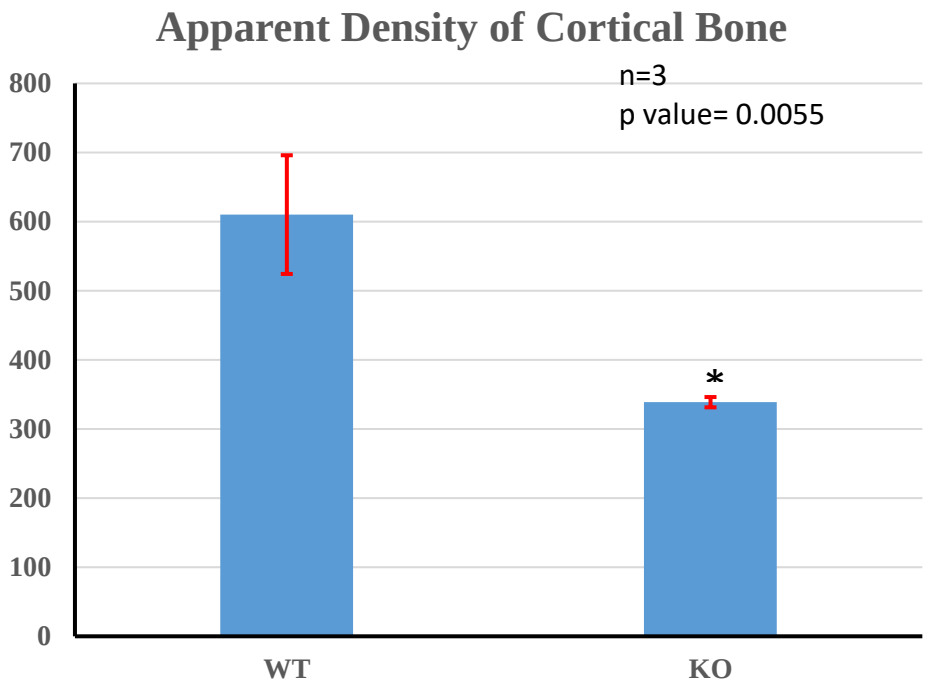

Figure 23. Apparent Density for Cortical Bone Graph: Quantitative analysis of Apparent density for cortical bone showed a statistically significant difference between control and KO samples (n=3, $P < 0.01$).

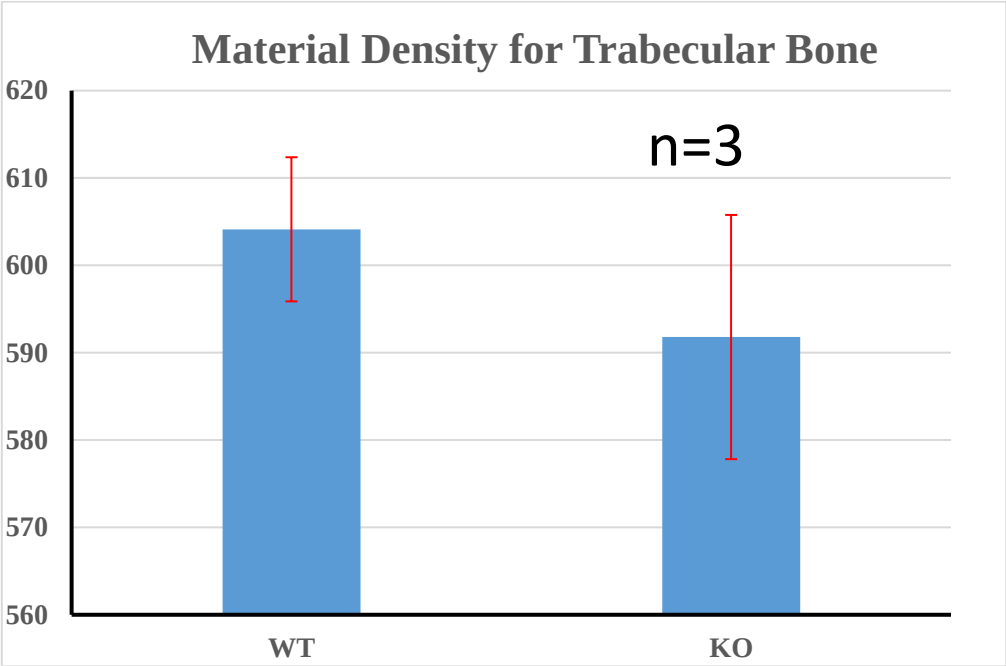

Figure 24. Material Density for Trabecular Bone Graph: Quantitative analysis of Apparent density for cortical bone showed no significant difference between control and KO samples (n=3, P > 0.05).

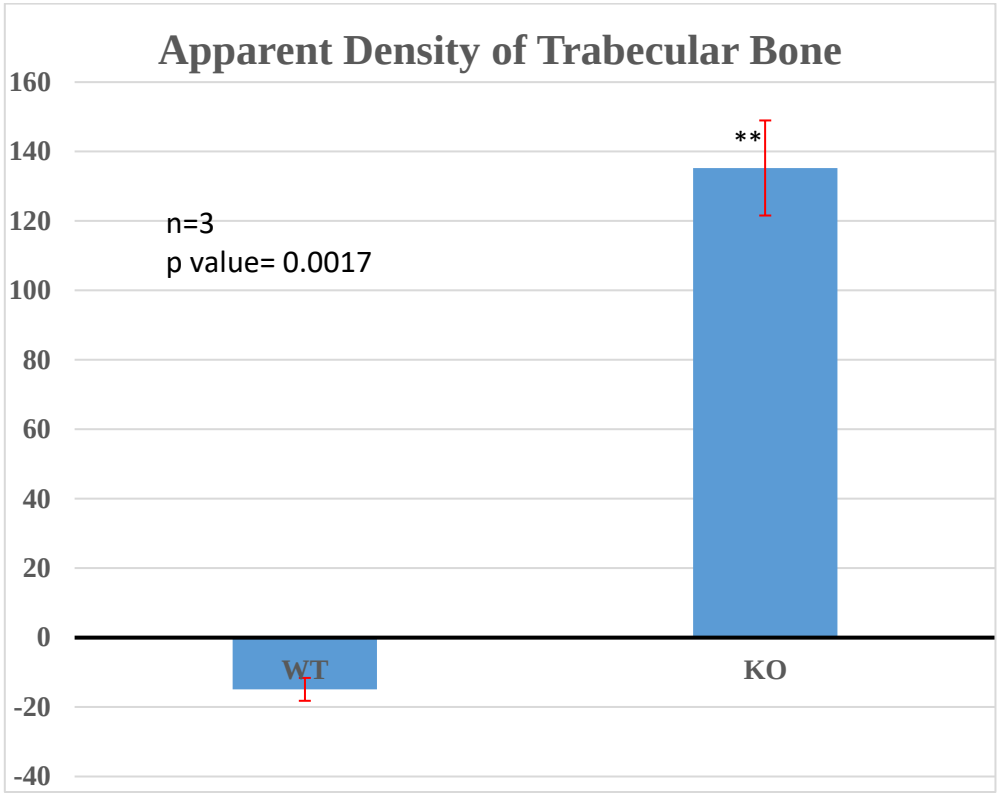

Figure 25. Apparent Density for Trabecular Bone Graph: Quantitative analysis of Apparent density for trabecular bone showed statistically significant difference between control and KO samples (n=3, $P < 0.01$).

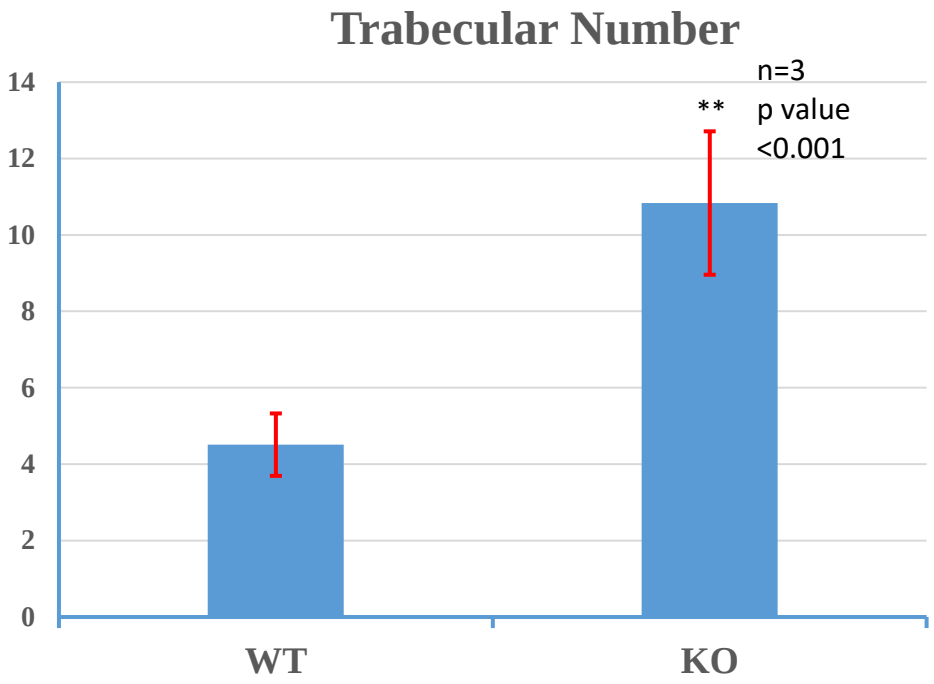

Figure 26. Trabecular number comparison graph: Quantitative analysis of trabecular number showed statistically significant differences between control and KO samples (n=3; P value < 0.001).

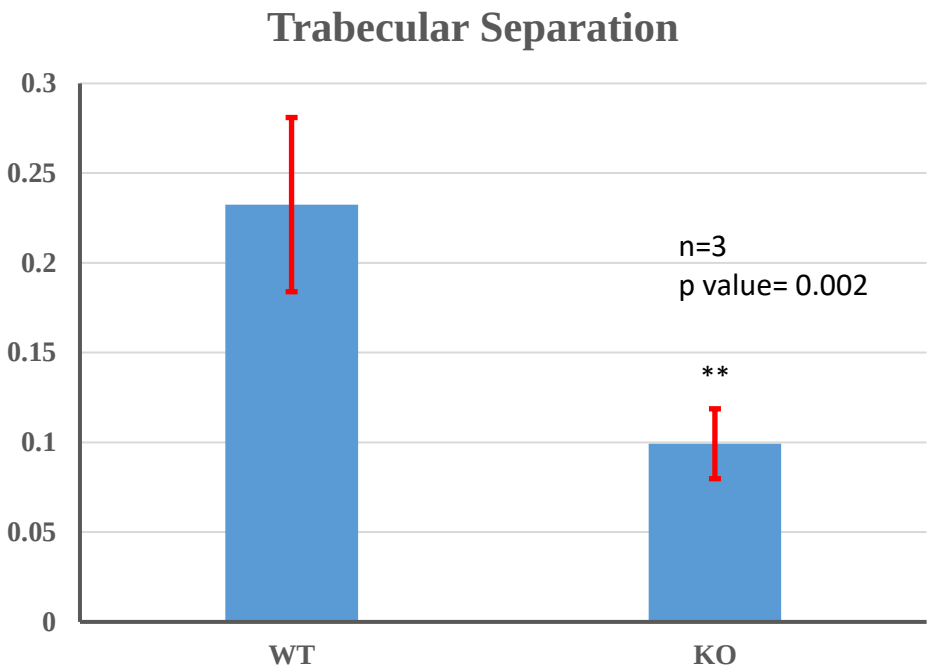

Figure 27. Trabecular separation comparison graph: Quantitative analysis of trabecular separation showed statistically significant differences between control and KO samples (n=3; P value < 0.01).

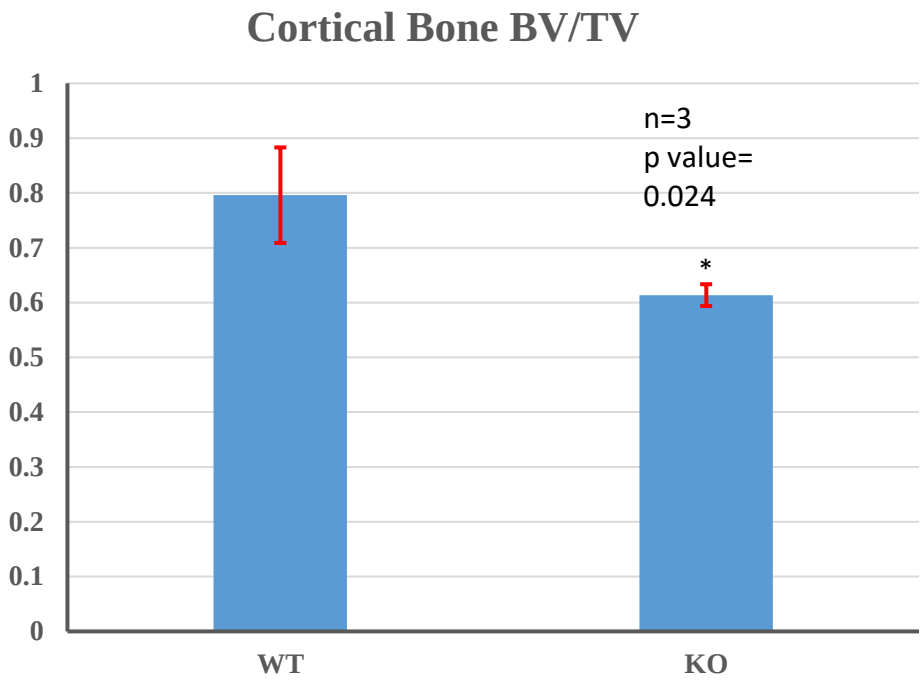

Figure 28. Cortical Bone BV/TV Graph: Quantitative analysis of cortical BV/TV showed statistically significant differences between control and KO samples (n=3; P value < 0.01).

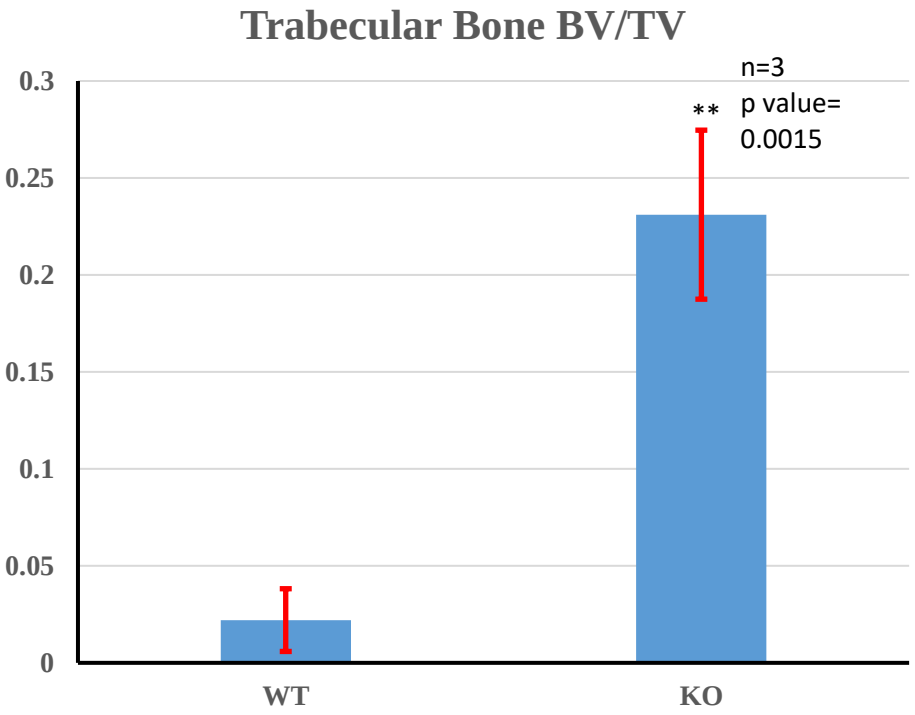

Figure 29. Trabecular bone BV/TV Graph: Quantitative analysis of trabecular BV/TV showed statistically significant differences between control and KO samples (n=3; P value < 0.01).

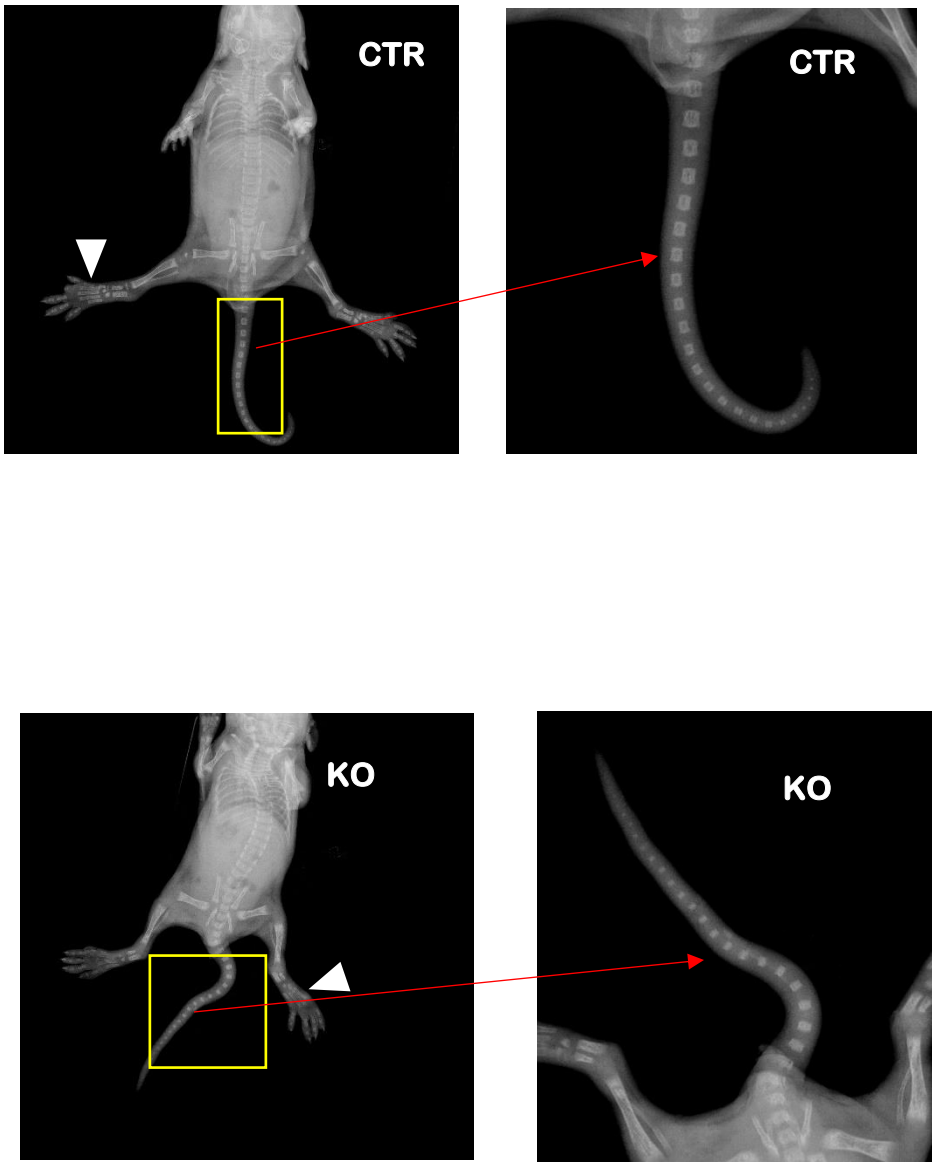

Figure 30. Metatarsal Radiographic Data: The white arrow heads are pointing to the metatarsals which are dissected and cultured for 8 days in culture medium. Of significance is the tail vertebra which are reduced in size in KO than Control mice (red arrows).

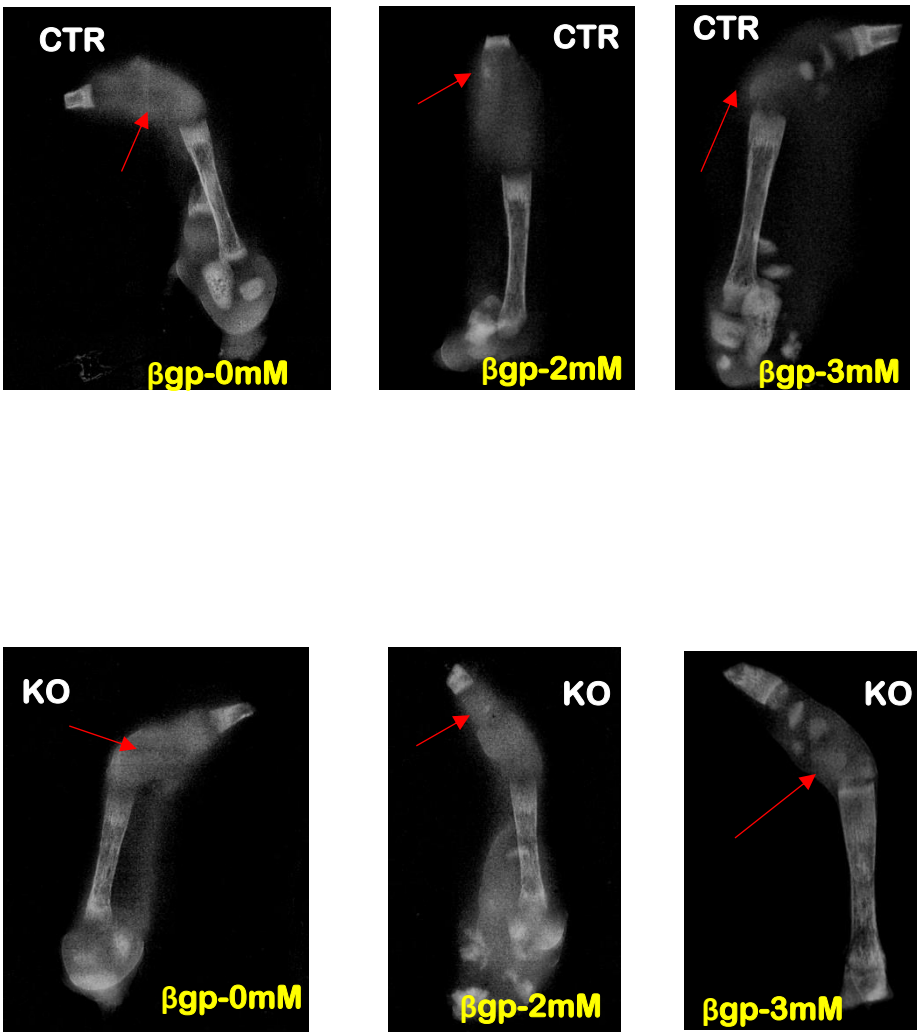

Figure 31. Metatarsal Organ Culture: The above figures represent with increase in phosphate concentration from 0milli Molar concentration to 3 millimolar concentration the secondary ossification center in epiphysis begins to form in the KO mice in the same manner as control in metatarsals in organ culture.

CHAPTER V
DISCUSSION

DMP1, a non-collagenous phosphoprotein, is highly expressed in osteocytes. The DMP1 mutation in humans or the deletion of Dmp1 in mice leads to ARHR (Feng et al., 2006; Ye et al., 2005). It is clear that a low phosphorous level is responsible for shortening of long bones and the delayed secondary ossification formation in Dmp1 null epiphyses. However, it is not understood why accumulation or 'persistence' of hypertrophic chondrocytes in the Dmp1 null growth plate occurs. One of the speculations was that the reduced apoptosis in the Dmp1 null hypertrophic chondrocytes leads to a failure in replacement of cartilage by bone tissue. Yet, this assumption cannot explain why there is more bone mass in the Dmp1 null metaphysis. In this study, cell lineage tracing technique was combined with multiple imaging and molecular study approaches to address why and how DMP1 null mice develop malformed long bones, in which there is an accumulated hyper chondrocyte layer and an expanded metaphysis. Key findings are (1) there is a sharp increase in the entire null cartilage layers, including proliferative, prehypertrophic, and hypertrophic zones of the growth plate (i.e., the low Pi level leads to more chondrocyte cell numbers); (2) there was an increase in Ki67 positive cells in null growth plate, suggesting that there is more cell proliferation in the null mice; (3) there was an increase in ALP activity in hypertrophic chondrocytes, suggesting a more active chondrocyte activity in the null mice; (4) there are more chondrocyte-derived bone cells with more

cartilage residues in the null metaphysis, indicating an acceleration of the cell transformation of chondrocytes into bone cells; (5) there is an increase in osteoblast bone markers such as COL1 and OPN expression but a great reduction in osteocyte markers like SOST in the null bone, indicating a defect in bone cell maturation; and (6) there is a unique role of Pi levels in epiphyses: a low Pi inhibits secondary ossification in vivo and an acceleration of the secondary ossification by Pi ex vivo, which raises an issue that Pi regulates the transformation from chondrocytes into bone cell in epiphyses in a different manner from that in the growth plate.

A notable and novel finding obtained in this study was that hypophosphatemia accelerates, instead of inhibits, chondrogenesis and the transformation of chondrocytes into bone cells in the growth plate. Because of a sharp acceleration in both chondrogenesis and osteogenesis in growth plates and metaphysis due to low Pi levels, cartilage matrices cannot be efficiently removed and the speed of maturation of osteoblasts into osteocytes cannot catch. As a result, the Dmp1 null mice display lengthened chondrocyte zones and expanded metaphysis with a great increase in immature osteoblasts and cartilage residues. Of note, this new finding does not exclude the impact of other factors (such as a moderate reduction in apoptosis and osteoclast number) on development of the Dmp1 null phenotype (Ye et al., 2005; R. Zhang et al., 2011). However, the potent role of a low Pi on chondrogenesis and cell transformation is the most critical cause for the growth plate and metaphysis null phenotype.

Because of free penetration of Pi through the placenta, the Dmp1 KO phenotype begins postnatally (Ye et al., 2005). Based on the ex vivo data (Fig 31), it is clear that secondary ossification formation is completely dose-dependent on phosphorus levels with no apparent difference between WT and KO metatarsals. Similar to growth plates, there are more active chondrogenesis in the KO than that in the WT epiphysis based on multiple assays described in (Figs 15a,17a – right panel) including Ki67 (reflecting cell proliferation), Col 2 (chondrocyte marker) and tomato (indicating chondrocyte activity). In contrast, there is a much smaller bone mass with fewer red bone cells in the KO epiphysis than that in the WT epiphysis. The bone markers such as Col 1, OPN and SOST are fewer in the KO epiphysis than those in the WT epiphysis (Figs 11a,12a,18a – right panel). These data seem to support the notion that a low level of Pi inhibits the cell transformation of chondrocytes into bone cells in the epiphysis. Although we do not understand why and how this inhibition occurs in the epiphysis, this unexpected event in the KO epiphysis may help explain why epiphysis development behinds metaphysis development in the same environment.

.

CHAPTER VI

CONCLUSIONS AND FUTURE DIRECTIONS

While the current dogma maintains that hypertrophic chondrocytes undergo apoptosis, recent evidence suggests otherwise i.e. that these chondrocytes directly transform into bone cells, rather than undergo apoptosis, during endochondral ossification. Using cell lineage tracing techniques in conventional knockout animal models such as the DMP1 knockout, can be explained the actual fate of hypertrophic chondrocytes in endochondral bone formation: in the conventional phenotype, these chondrocytes seem to differentiate into immature bone cells and form bone relatively early, as evidenced by shorter-than-normal or 'stunted' long bones presenting with marked metaphyseal expansion in the metaphysis but the cell transformation seems to be affected in epiphysis which explains why there is delayed secondary ossification in epiphysis in the same low phosphate environment despite accelerated chondrogenesis.. However, further elucidation on the genetic and molecular underpinnings, and mechanisms, that consign chondrocytes to such fate (during endochondral bone development) is needed.

Future directions include analyzing the effect of high phosphate on skeleton, developmentally, at 3 weeks, 7 weeks and 3 months.

Three-week-old mice will subsist on a phosphate-rich diet over the next 4 weeks and then sacrificed at 7 weeks of age. Similarly, 2-month-old mice will be given tamoxifen to activate Aggcrecan cre after which they subsist on a phosphate-rich diet over 4 weeks, and, at 3 months of age, will be sacrificed.

Using this approach, the effect of high phosphate on cell transformation can be more selectively traced in both epiphysis and metaphysis.

REFERENCES

A, P. (1991). Cartilage: "Molecular Aspects". Boca Raton, Florida: CRC press.

Agger, K., Cloos, P. A., Christensen, J., Pasini, D., Rose, S., Rappsilber, J., . . . Helin, K. (2007). UTX and JMJD3 are histone H3K27 demethylases involved in HOX gene regulation and development. *Nature, 449*(7163), 731-734. doi:10.1038/nature06145

Akiyama, H., Chaboissier, M. C., Martin, J. F., Schedl, A., & de Crombrugghe, B. (2002). The transcription factor Sox9 has essential roles in successive steps of the chondrocyte differentiation pathway and is required for expression of Sox5 and Sox6. *Genes Dev, 16*(21), 2813-2828. doi:10.1101/gad.1017802

Bastepe, M., Weinstein, L. S., Ogata, N., Kawaguchi, H., Juppner, H., Kronenberg, H. M., & Chung, U. I. (2004). Stimulatory G protein directly regulates hypertrophic differentiation of growth plate cartilage in vivo. *Proc Natl Acad Sci U S A, 101*(41), 14794-14799. doi:10.1073/pnas.0405091101

Bi, W., Deng, J. M., Zhang, Z., Behringer, R. R., & de Crombrugghe, B. (1999). Sox9 is required for cartilage formation. *Nat Genet, 22*(1), 85-89. doi:10.1038/8792

Bingham, P. J., & Raisz, L. G. (1974). Bone growth in organ culture: effects of phosphate and other nutrients on bone and cartilage. *Calcif Tissue Res, 14*(1), 31-48.

Chang, A. C., Janosi, J., Hulsbeek, M., de Jong, D., Jeffrey, K. J., Noble, J. R., & Reddel, R. R. (1995). A novel human cDNA highly homologous to the fish hormone stanniocalcin. *Mol Cell Endocrinol, 112*(2), 241-247.

Chung, U. I., Lanske, B., Lee, K., Li, E., & Kronenberg, H. (1998). The parathyroid hormone/parathyroid hormone-related peptide receptor coordinates endochondral bone development by directly controlling chondrocyte differentiation. *Proc Natl Acad Sci U S A, 95*(22), 13030-13035.

Chung, U. I., Schipani, E., McMahon, A. P., & Kronenberg, H. M. (2001). Indian hedgehog couples chondrogenesis to osteogenesis in endochondral bone development. *J Clin Invest, 107*(3), 295-304. doi:10.1172/jci11706

Colvin, J. S., Bohne, B. A., Harding, G. W., McEwen, D. G., & Ornitz, D. M. (1996). Skeletal overgrowth and deafness in mice lacking fibroblast growth factor receptor 3. *Nat Genet, 12*(4), 390-397. doi:10.1038/ng0496-390

Czermin, B., Melfi, R., McCabe, D., Seitz, V., Imhof, A., & Pirrotta, V. (2002). Drosophila enhancer of Zeste/ESC complexes have a histone H3 methyltransferase activity that marks chromosomal Polycomb sites. *Cell, 111*(2), 185-196.

Day, T. F., Guo, X., Garrett-Beal, L., & Yang, Y. (2005). Wnt/beta-catenin signaling in mesenchymal progenitors controls osteoblast and chondrocyte differentiation during vertebrate skeletogenesis. *Dev Cell, 8*(5), 739-750. doi:10.1016/j.devcel.2005.03.016

de Crombrugghe, B., Lefebvre, V., & Nakashima, K. (2001). Regulatory mechanisms in the pathways of cartilage and bone formation. *Curr Opin Cell Biol, 13*(6), 721-727.

De Niu, P., Radman, D. P., Jaworski, E. M., Deol, H., Gentz, R., Su, J., . . . Wagner, G. F. (2000). Development of a human stanniocalcin radioimmunoassay: serum and tissue hormone levels and pharmacokinetics in the rat. *Mol Cell Endocrinol, 162*(1-2), 131-144.

De Santa, F., Totaro, M. G., Prosperini, E., Notarbartolo, S., Testa, G., & Natoli, G. (2007). The histone H3 lysine-27 demethylase Jmjd3 links inflammation to inhibition of polycomb-mediated gene silencing. *Cell, 130*(6), 1083-1094. doi:10.1016/j.cell.2007.08.019

Deak, F., Wagener, R., Kiss, I., & Paulsson, M. (1999). The matrilins: a novel family of oligomeric extracellular matrix proteins. *Matrix Biol, 18*(1), 55-64.

Deng, C., Wynshaw-Boris, A., Zhou, F., Kuo, A., & Leder, P. (1996). Fibroblast growth factor receptor 3 is a negative regulator of bone growth. *Cell, 84*(6), 911-921.

Ducy, P., Zhang, R., Geoffroy, V., Ridall, A. L., & Karsenty, G. (1997). Osf2/Cbfa1: a transcriptional activator of osteoblast differentiation. *Cell, 89*(5), 747-754.

Enomoto-Iwamoto, M., Enomoto, H., Komori, T., & Iwamoto, M. (2001). Participation of Cbfa1 in regulation of chondrocyte maturation. *Osteoarthritis Cartilage, 9 Suppl A*, S76-84.

Enomoto, H., Enomoto-Iwamoto, M., Iwamoto, M., Nomura, S., Himeno, M., Kitamura, Y., . . . Komori, T. (2000). Cbfa1 is a positive regulatory factor in chondrocyte maturation. *J Biol Chem, 275*(12), 8695-8702.

Feng, J. Q., Ward, L. M., Liu, S., Lu, Y., Xie, Y., Yuan, B., . . . White, K. E. (2006). Loss of DMP1 causes rickets and osteomalacia and identifies a role for osteocytes in mineral metabolism. *Nat Genet, 38*(11), 1310-1315. doi:10.1038/ng1905

Fisher LW, F. N. (2003). Six genes expressed in bones and teeth encode the current members of the SIBLING family of proteins. *Connective tissue research, 44*(Suppl 1), 33-40.

Fresquet, M., Jowitt, T. A., Ylostalo, J., Coffey, P., Meadows, R. S., Ala-Kokko, L., . . . Briggs, M. D. (2007). Structural and functional characterization of recombinant matrilin-3 A-domain and implications for human genetic bone diseases. *J Biol Chem, 282*(48), 34634-34643. doi:10.1074/jbc.M705301200

Fujita, T., Izumo, N., Fukuyama, R., Meguro, T., Nakamuta, H., Kohno, T., & Koida, M. (2001). Phosphate provides an extracellular signal that drives nuclear export of Runx2/Cbfa1 in bone cells. *Biochem Biophys Res Commun, 280*(1), 348-352. doi:10.1006/bbrc.2000.4108

Goldring, M. B., Tsuchimochi, K., & Ijiri, K. (2006). The control of chondrogenesis. *J Cell Biochem, 97*(1), 33-44. doi:10.1002/jcb.20652

Gonzalez, G. A., & Montminy, M. R. (1989). Cyclic AMP stimulates somatostatin gene transcription by phosphorylation of CREB at serine 133. *Cell, 59*(4), 675-680.

Graham, A., Francis-West, P., Brickell, P., & Lumsden, A. (1994). The signalling molecule BMP4 mediates apoptosis in the rhombencephalic neural crest. *Nature, 372*(6507), 684-686. doi:10.1038/372684a0

Guo, J., Chung, U. I., Kondo, H., Bringhurst, F. R., & Kronenberg, H. M. (2002). The PTH/PTHrP receptor can delay chondrocyte hypertrophy in vivo without activating phospholipase C. *Dev Cell, 3*(2), 183-194.

Guo, X., Day, T. F., Jiang, X., Garrett-Beal, L., Topol, L., & Yang, Y. (2004). Wnt/beta-catenin signaling is sufficient and necessary for synovial joint formation. *Genes Dev, 18*(19), 2404-2417. doi:10.1101/gad.1230704

Henry, S. P., Jang, C. W., Deng, J. M., Zhang, Z., Behringer, R. R., & de Crombrugghe, B. (2009). Generation of aggrecan-CreERT2 knockin mice for inducible Cre activity in adult cartilage. *Genesis, 47*(12), 805-814. doi:10.1002/dvg.20564

Hong, S., Cho, Y. W., Yu, L. R., Yu, H., Veenstra, T. D., & Ge, K. (2007). Identification of JmjC domain-containing UTX and JMJD3 as histone H3 lysine 27 demethylases. *Proc Natl Acad Sci U S A, 104*(47), 18439-18444. doi:10.1073/pnas.0707292104

Hoshi, K., Komori, T., & Ozawa, H. (1999). Morphological characterization of skeletal cells in Cbfa1-deficient mice. *Bone, 25*(6), 639-651.

Howell, D. S., Pita, J. C., Marquez, J. F., & Madruga, J. E. (1968). Partition of calcium, phosphate, and protein in the fluid phase aspirated at calcifying sites in epiphyseal cartilage. *J Clin Invest, 47*(5), 1121-1132. doi:10.1172/jci105801

Jayasuriya, C. T., Goldring, M. B., Terek, R., & Chen, Q. (2012). Matrilin-3 induction of IL-1 receptor antagonist is required for up-regulating collagen II and aggrecan and down-regulating ADAMTS-5 gene expression. *Arthritis Res Ther, 14*(5), R197. doi:10.1186/ar4033

Jing, Y., Zhou, X., Han, X., Jing, J., von der Mark, K., Wang, J., . . . Feng, J. Q. (2015). Chondrocytes Directly Transform into Bone Cells in Mandibular Condyle Growth. *J Dent Res, 94*(12), 1668-1675. doi:10.1177/0022034515598135

Kakuta, S., Golub, E. E., & Shapiro, I. M. (1985). Morphochemical analysis of phosphorus pools in calcifying cartilage. *Calcif Tissue Int, 37*(3), 293-299.

Karaplis, A. C., Luz, A., Glowacki, J., Bronson, R. T., Tybulewicz, V. L., Kronenberg, H. M., & Mulligan, R. C. (1994). Lethal skeletal dysplasia from targeted disruption of the parathyroid hormone-related peptide gene. *Genes Dev, 8*(3), 277-289.

Karp, S. J., Schipani, E., St-Jacques, B., Hunzelman, J., Kronenberg, H., & McMahon, A. P. (2000). Indian hedgehog coordinates endochondral bone growth and morphogenesis via parathyroid hormone related-protein-dependent and -independent pathways. *Development, 127*(3), 543-548.

Kato, M., Patel, M. S., Levasseur, R., Lobov, I., Chang, B. H., Glass, D. A., 2nd, . . . Chan, L. (2002). Cbfa1-independent decrease in osteoblast proliferation, osteopenia, and persistent embryonic eye vascularization in mice deficient in Lrp5, a Wnt coreceptor. *J Cell Biol, 157*(2), 303-314. doi:10.1083/jcb.200201089

Kim, I. S., Otto, F., Zabel, B., & Mundlos, S. (1999). Regulation of chondrocyte differentiation by Cbfa1. *Mech Dev, 80*(2), 159-170.

Kingsley, D. M. (1994). What do BMPs do in mammals? Clues from the mouse short-ear mutation. *Trends Genet, 10*(1), 16-21.

Klatt, A. R., Nitsche, D. P., Kobbe, B., Morgelin, M., Paulsson, M., & Wagener, R. (2000). Molecular structure and tissue distribution of matrilin-3, a filament-forming extracellular matrix protein expressed during skeletal development. *J Biol Chem, 275*(6), 3999-4006.

Kobayashi, T., Chung, U. I., Schipani, E., Starbuck, M., Karsenty, G., Katagiri, T., . . . Kronenberg, H. M. (2002). PTHrP and Indian hedgehog control differentiation of growth plate chondrocytes at multiple steps. *Development, 129*(12), 2977-2986.

Komori, T., Yagi, H., Nomura, S., Yamaguchi, A., Sasaki, K., Deguchi, K., . . . Kishimoto, T. (1997). Targeted disruption of Cbfa1 results in a complete lack of bone formation owing to maturational arrest of osteoblasts. *Cell, 89*(5), 755-764.

Kronenberg, H. M. (2003). Developmental regulation of the growth plate. *Nature, 423*(6937), 332-336. doi:10.1038/nature01657

Kubicek, S., & Jenuwein, T. (2004). A crack in histone lysine methylation. *Cell, 119*(7), 903-906. doi:10.1016/j.cell.2004.12.006

Kugimiya, F., Kawaguchi, H., Kamekura, S., Chikuda, H., Ohba, S., Yano, F., . . . Chung, U. I. (2005). Involvement of endogenous bone morphogenetic protein (BMP) 2 and BMP6 in bone formation. *J Biol Chem, 280*(42), 35704-35712. doi:10.1074/jbc.M505166200

Lanske, B., Karaplis, A. C., Lee, K., Luz, A., Vortkamp, A., Pirro, A., . . . Kronenberg, H. M. (1996). PTH/PTHrP receptor in early development and Indian hedgehog-regulated bone growth. *Science, 273*(5275), 663-666.

Leboy, P., Grasso-Knight, G., D'Angelo, M., Volk, S. W., Lian, J. V., Drissi, H., . . . Adams, S. L. (2001). Smad-Runx interactions during chondrocyte maturation. *J Bone Joint Surg Am, 83-A Suppl 1*(Pt 1), S15-22.

Lefebvre, V., Huang, W., Harley, V. R., Goodfellow, P. N., & de Crombrugghe, B. (1997). SOX9 is a potent activator of the chondrocyte-specific enhancer of the pro alpha1(II) collagen gene. *Mol Cell Biol, 17*(4), 2336-2346.

Li, X., Schwarz, E. M., Zuscik, M. J., Rosier, R. N., Ionescu, A. M., Puzas, J. E., . . . O'Keefe, R. J. (2003). Retinoic acid stimulates chondrocyte differentiation and enhances bone morphogenetic protein effects through induction of Smad1 and Smad5. *Endocrinology, 144*(6), 2514-2523. doi:10.1210/en.2002-220969

Lin, S., Zhang, Q., Cao, Z., Lu, Y., Zhang, H., Yan, K., . . . Feng, J. Q. (2014). Constitutive nuclear expression of dentin matrix protein 1 fails to rescue the Dmp1-null phenotype. *J Biol Chem, 289*(31), 21533-21543. doi:10.1074/jbc.M113.543330

Liu, S., Zhou, J., Tang, W., Menard, R., Feng, J. Q., & Quarles, L. D. (2008). Pathogenic role of Fgf23 in Dmp1-null mice. *Am J Physiol Endocrinol Metab, 295*(2), E254-261. doi:10.1152/ajpendo.90201.2008

Logan, C. Y., & Nusse, R. (2004). The Wnt signaling pathway in development and disease. *Annu Rev Cell Dev Biol, 20*, 781-810. doi:10.1146/annurev.cellbio.20.010403.113126

Lu, M., Wagner, G. F., & Renfro, J. L. (1994). Stanniocalcin stimulates phosphate reabsorption by flounder renal proximal tubule in primary culture. *Am J Physiol, 267*(5 Pt 2), R1356-1362.

Madsen, K. L., Tavernini, M. M., Yachimec, C., Mendrick, D. L., Alfonso, P. J., Buergin, M., . . . Fedorak, R. N. (1998). Stanniocalcin: a novel protein regulating calcium and phosphate transport across mammalian intestine. *Am J Physiol, 274*(1 Pt 1), G96-102.

Magne, D., Bluteau, G., Faucheux, C., Palmer, G., Vignes-Colombeix, C., Pilet, P., . . . Guicheux, J. (2003). Phosphate is a specific signal for ATDC5 chondrocyte maturation and apoptosis-associated mineralization: possible implication of apoptosis in the regulation of endochondral ossification. *J Bone Miner Res, 18*(8), 1430-1442. doi:10.1359/jbmr.2003.18.8.1430

Makras, P., Hamdy, N. A., Kant, S. G., & Papapoulos, S. E. (2008). Normal growth and muscle dysfunction in X-linked hypophosphatemic rickets associated with a novel mutation in the PHEX gene. *J Clin Endocrinol Metab, 93*(4), 1386-1389. doi:10.1210/jc.2007-1296

Mansfield, K., Rajpurohit, R., & Shapiro, I. M. (1999). Extracellular phosphate ions cause apoptosis of terminally differentiated epiphyseal chondrocytes. *J Cell Physiol, 179*(3), 276-286. doi:10.1002/(sici)1097-4652(199906)179:3<276::aid-jcp5>3.0.co;2-#

Mansfield, K., Teixeira, C. C., Adams, C. S., & Shapiro, I. M. (2001). Phosphate ions mediate chondrocyte apoptosis through a plasma membrane transporter mechanism. *Bone, 28*(1), 1-8.

Mantovani, G., Spada, A., & Elli, F. M. (2016). Pseudohypoparathyroidism and Gsalpha-cAMP-linked disorders: current view and open issues. *Nat Rev Endocrinol, 12*(6), 347-356. doi:10.1038/nrendo.2016.52

Martin, C., & Zhang, Y. (2005). The diverse functions of histone lysine methylation. *Nat Rev Mol Cell Biol, 6*(11), 838-849. doi:10.1038/nrm1761

Massague, J. (2012). TGFbeta signalling in context. *Nat Rev Mol Cell Biol, 13*(10), 616-630. doi:10.1038/nrm3434

Massague, J., & Wotton, D. (2000). Transcriptional control by the TGF-beta/Smad signaling system. *Embo j, 19*(8), 1745-1754. doi:10.1093/emboj/19.8.1745

Muller, J., Hart, C. M., Francis, N. J., Vargas, M. L., Sengupta, A., Wild, B., . . . Simon, J. A. (2002). Histone methyltransferase activity of a Drosophila Polycomb group repressor complex. *Cell, 111*(2), 197-208.

Mundlos, S., Huang, L. F., Selby, P., & Olsen, B. R. (1996). Cleidocranial dysplasia in mice. *Ann N Y Acad Sci, 785*, 301-302.

Olsen, H. S., Cepeda, M. A., Zhang, Q. Q., Rosen, C. A., Vozzolo, B. L., & Wagner, G. F. (1996). Human stanniocalcin: a possible hormonal regulator of mineral metabolism. *Proc Natl Acad Sci U S A, 93*(5), 1792-1796.

Otto, F., Thornell, A. P., Crompton, T., Denzel, A., Gilmour, K. C., Rosewell, I. R., . . . Owen, M. J. (1997). Cbfa1, a candidate gene for cleidocranial dysplasia syndrome,

is essential for osteoblast differentiation and bone development. *Cell, 89*(5), 765-771.

Parr, B. A., Shea, M. J., Vassileva, G., & McMahon, A. P. (1993). Mouse Wnt genes exhibit discrete domains of expression in the early embryonic CNS and limb buds. *Development, 119*(1), 247-261.

Pei, M., Luo, J., & Chen, Q. (2008). Enhancing and maintaining chondrogenesis of synovial fibroblasts by cartilage extracellular matrix protein matrilins. *Osteoarthritis Cartilage, 16*(9), 1110-1117. doi:10.1016/j.joca.2007.12.011

Rajpurohit, R., Mansfield, K., Ohyama, K., Ewert, D., & Shapiro, I. M. (1999). Chondrocyte death is linked to development of a mitochondrial membrane permeability transition in the growth plate. *J Cell Physiol, 179*(3), 287-296. doi:10.1002/(sici)1097-4652(199906)179:3<287::aid-jcp6>3.0.co;2-t

Rudolph, D., Tafuri, A., Gass, P., Hammerling, G. J., Arnold, B., & Schutz, G. (1998). Impaired fetal T cell development and perinatal lethality in mice lacking the cAMP response element binding protein. *Proc Natl Acad Sci U S A, 95*(8), 4481-4486.

Sabbagh, Y., Carpenter, T. O., & Demay, M. B. (2005). Hypophosphatemia leads to rickets by impairing caspase-mediated apoptosis of hypertrophic chondrocytes. *Proc Natl Acad Sci U S A, 102*(27), 9637-9642. doi:10.1073/pnas.0502249102

Saito, H., Kusano, K., Kinosaki, M., Ito, H., Hirata, M., Segawa, H., . . . Fukushima, N. (2003). Human fibroblast growth factor-23 mutants suppress Na+-dependent phosphate co-transport activity and 1alpha,25-dihydroxyvitamin D3 production. *J Biol Chem, 278*(4), 2206-2211. doi:10.1074/jbc.M207872200

Sakamoto, A., Chen, M., Kobayashi, T., Kronenberg, H. M., & Weinstein, L. S. (2005). Chondrocyte-specific knockout of the G protein G(s)alpha leads to epiphyseal and growth plate abnormalities and ectopic chondrocyte formation. *J Bone Miner Res, 20*(4), 663-671. doi:10.1359/jbmr.041210

Schiavi, S. C., & Kumar, R. (2004). The phosphatonin pathway: new insights in phosphate homeostasis. *Kidney Int, 65*(1), 1-14. doi:10.1111/j.1523-1755.2004.00355.x

Shen, R., Jia, R., Liu, W., Lin, Q., Hai, Y., & He, Z. (2015). The Function and Regulation of BMP6 in Various Kinds of Stem Cells. *Curr Pharm Des, 21*(25), 3634-3643.

Shimada, T., Mizutani, S., Muto, T., Yoneya, T., Hino, R., Takeda, S., . . . Yamashita, T. (2001). Cloning and characterization of FGF23 as a causative factor of tumor-induced osteomalacia. *Proc Natl Acad Sci U S A, 98*(11), 6500-6505. doi:10.1073/pnas.101545198

Soriano, P. (1999). Generalized lacZ expression with the ROSA26 Cre reporter strain. *Nat Genet, 21*(1), 70-71. doi:10.1038/5007

Strahl, B. D., & Allis, C. D. (2000). The language of covalent histone modifications. *Nature, 403*(6765), 41-45. doi:10.1038/47412

Tenenhouse, H. S. (1997). Cellular and molecular mechanisms of renal phosphate transport. *J Bone Miner Res, 12*(2), 159-164. doi:10.1359/jbmr.1997.12.2.159

Tu, Q., Pi, M., Karsenty, G., Simpson, L., Liu, S., & Quarles, L. D. (2003). Rescue of the skeletal phenotype in CasR-deficient mice by transfer onto the Gcm2 null background. *J Clin Invest, 111*(7), 1029-1037. doi:10.1172/jci17054

Turan, S., & Bastepe, M. (2015). GNAS Spectrum of Disorders. *Curr Osteoporos Rep, 13*(3), 146-158. doi:10.1007/s11914-015-0268-x

Vega, R. B., Matsuda, K., Oh, J., Barbosa, A. C., Yang, X., Meadows, E., . . . Olson, E. N. (2004). Histone deacetylase 4 controls chondrocyte hypertrophy during skeletogenesis. *Cell, 119*(4), 555-566. doi:10.1016/j.cell.2004.10.024

Vortkamp, A., Lee, K., Lanske, B., Segre, G. V., Kronenberg, H. M., & Tabin, C. J. (1996). Regulation of rate of cartilage differentiation by Indian hedgehog and PTH-related protein. *Science, 273*(5275), 613-622.

Wagener, R., Kobbe, B., & Paulsson, M. (1997). Primary structure of matrilin-3, a new member of a family of extracellular matrix proteins related to cartilage matrix protein (matrilin-1) and von Willebrand factor. *FEBS Lett, 413*(1), 129-134.

Wagner, G. F., Guiraudon, C. C., Milliken, C., & Copp, D. H. (1995). Immunological and biological evidence for a stanniocalcin-like hormone in human kidney. *Proc Natl Acad Sci U S A, 92*(6), 1871-1875.

Wagner, G. F., Hampong, M., Park, C. M., & Copp, D. H. (1986). Purification, characterization, and bioassay of teleocalcin, a glycoprotein from salmon corpuscles of Stannius. *Gen Comp Endocrinol, 63*(3), 481-491.

Wagner, G. F., Milliken, C., Friesen, H. G., & Copp, D. H. (1991). Studies on the regulation and characterization of plasma stanniocalcin in rainbow trout. *Mol Cell Endocrinol, 79*(1-3), 129-138.

Wagner, G. F., Vozzolo, B. L., Jaworski, E., Haddad, M., Kline, R. L., Olsen, H. S., . . . Renfro, J. L. (1997). Human stanniocalcin inhibits renal phosphate excretion in the rat. *J Bone Miner Res, 12*(2), 165-171. doi:10.1359/jbmr.1997.12.2.165

Worthington, R. A., Brown, L., Jellinek, D., Chang, A. C., Reddel, R. R., Hambly, B. D., & Barden, J. A. (1999). Expression and localisation of stanniocalcin 1 in rat bladder, kidney and ovary. *Electrophoresis, 20*(10), 2071-2076. doi:10.1002/(sici)1522-2683(19990701)20:10<2071::aid-elps2071>3.0.co;2-#

Yamashita, T., Yoshioka, M., & Itoh, N. (2000). Identification of a novel fibroblast growth factor, FGF-23, preferentially expressed in the ventrolateral thalamic nucleus of the brain. *Biochem Biophys Res Commun, 277*(2), 494-498. doi:10.1006/bbrc.2000.3696

Yang, D., Okamura, H., Nakashima, Y., & Haneji, T. (2013). Histone demethylase Jmjd3 regulates osteoblast differentiation via transcription factors Runx2 and osterix. *J Biol Chem, 288*(47), 33530-33541. doi:10.1074/jbc.M113.497040

Yang, G., Cui, F., Hou, N., Cheng, X., Zhang, J., Wang, Y., . . . Yang, X. (2005). Transgenic mice that express Cre recombinase in hypertrophic chondrocytes. *Genesis, 42*(1), 33-36. doi:10.1002/gene.20120

Ye, L., Mishina, Y., Chen, D., Huang, H., Dallas, S. L., Dallas, M. R., . . . Feng, J. Q. (2005). Dmp1-deficient mice display severe defects in cartilage formation responsible for a chondrodysplasia-like phenotype. *J Biol Chem, 280*(7), 6197-6203. doi:10.1074/jbc.M412911200

Yuan, B., Takaiwa, M., Clemens, T. L., Feng, J. Q., Kumar, R., Rowe, P. S., . . . Drezner, M. K. (2008). Aberrant Phex function in osteoblasts and osteocytes alone underlies murine X-linked hypophosphatemia. *J Clin Invest, 118*(2), 722-734. doi:10.1172/jci32702

Zalutskaya, A. A., Cox, M. K., & Demay, M. B. (2009). Phosphate regulates embryonic endochondral bone development. *J Cell Biochem, 108*(3), 668-674. doi:10.1002/jcb.22302

Zhang, F., Xu, L., Xu, L., Xu, Q., Li, D., Yang, Y., . . . Chen, C. D. (2015). JMJD3 promotes chondrocyte proliferation and hypertrophy during endochondral bone formation in mice. *J Mol Cell Biol, 7*(1), 23-34. doi:10.1093/jmcb/mjv003

Zhang, R., Lu, Y., Ye, L., Yuan, B., Yu, S., Qin, C., . . . Feng, J. Q. (2011). Unique roles of phosphorus in endochondral bone formation and osteocyte maturation. *J Bone Miner Res, 26*(5), 1047-1056. doi:10.1002/jbmr.294

Zou, H., & Niswander, L. (1996). Requirement for BMP signaling in interdigital apoptosis and scale formation. *Science, 272*(5262), 738-741.